NUREG/CR-1801
ANL-80-107

NUREG/CR-1801
ANL-80-107

MASTER

LIGHT-WATER-REACTOR SAFETY RESEARCH PROGRAM: QUARTERLY PROGRESS REPORT

April—June 1980

ARGONNE NATIONAL LABORATORY, ARGONNE, ILLINOIS

Prepared for the U. S. NUCLEAR REGULATORY COMMISSION
under Interagency Agreement DOE 40-550-75

The facilities of Argonne National Laboratory are owned by the United States Government. Under the terms of a contract (W-31-109-Eng-38) among the U. S. Department of Energy, Argonne Universities Association and The University of Chicago, the University employs the staff and operates the Laboratory in accordance with policies and programs formulated, approved and reviewed by the Association.

MEMBERS OF ARGONNE UNIVERSITIES ASSOCIATION

The University of Arizona
Carnegie-Mellon University
Case Western Reserve University
The University of Chicago
University of Cincinnati
Illinois Institute of Technology
University of Illinois
Indiana University
The University of Iowa
Iowa State University
The University of Kansas
Kansas State University
Loyola University of Chicago
Marquette University
The University of Michigan
Michigan State University
University of Minnesota
University of Missouri
Northwestern University
University of Notre Dame
The Ohio State University
Ohio University
The Pennsylvania State University
Purdue University
Saint Louis University
Southern Illinois University
The University of Texas at Austin
Washington University
Wayne State University
The University of Wisconsin-Madison

Available from

GPO Sales Program
Division of Technical Information and Document Control
U. S. Nuclear Regulatory Commission
Washington, D.C. 20555

and

National Technical Information Service
Springfield, Virginia 22161

NUREG/CR-1801
ANL-80-107

(Distribution
Code: R3)

ARGONNE NATIONAL LABORATORY
9700 South Cass Avenue
Argonne, Illinois 60439

NUREG/CR--1801

TI85 015883

LIGHT-WATER-REACTOR SAFETY RESEARCH PROGRAM: QUARTERLY PROGRESS REPORT

April-June 1980

by

Walter E. Massey, Laboratory Director
Charles E. Till, Associate Laboratory Director

Date Published: October 1980

Previous reports in this series

ANL-79-81	April-June 1979
ANL-79-108	July-September 1979
ANL-80-43	October-December 1979
ANL-80-86	January-March 1980

Prepared for the Division of Reactor Safety Research
Office of Nuclear Regulatory Research
U. S. Nuclear Regulatory Commission
Washington, D.C. 20555
Under Interagency Agreement DOE 40-550-75

NRC FIN No. A2016

LIGHT-WATER-REACTOR SAFETY
RESEARCH PROGRAM:
QUARTERLY PROGRESS REPORT

April-June 1980

ABSTRACT

This progress report summarizes the Argonne National Laboratory work performed during April, May, and June 1980 on water-reactor-safety problems. The research and development area covered is Transient Fuel Response and Fission-product Release.

NRC FIN No.	FIN Title
A2016	Transient Fuel Response and Fission-product Release

TABLE OF CONTENTS

LIGHT-WATER-REACTOR SAFETY
RESEARCH PROGRAM:
QUARTERLY PROGRESS REPORT

April-June 1980

EXECUTIVE SUMMARY

Parametric correlations of two and three variables have been developed to describe GRASS-SST-predicted steady-state fission-gas release from UO_2-based fuels. The parametric model, PARAGRASS, has the capability of reproducing GRASS-SST results with good accuracy. In future work, other parameters will be included in the model, and the model will be extended to transient analyses. Also, the methods used to develop correlations for fission-gas release will be used to develop correlations for fuel-swelling strain. An assumption used in the GRASS-SST calculation of grain-edge swelling has been found deficient and is being replaced with a more realistic model.

Specimens from the ORNL program "Fission Product Behavior in LWRs" were sent to ANL-East for a determination of the mechanism of fission-product release during the high-temperature (>1300°C) tests. The preliminary examination of the specimens has been completed. Intergranular microcracking occurred during the tests at temperatures greater than 1400°C, and presumably made an important contribution to the observed release of fission products.

A second phenomenon observed in the high-temperature tests is the reaction of UO_2 and Zircaloy to form a liquid-phase reaction product. This reaction caused the release of additional fission products. Further study of the UO_2-Zircaloy reaction product is planned because of its importance to the understanding of the TMI-2 accident.

TRANSIENT FUEL RESPONSE AND FISSION-PRODUCT RELEASE

Principal Investigators:
J. Rest and S. M. Gehl, MSD

A. Introduction and Summary

A physically realistic description of fuel swelling and fission-gas release is needed to aid in predicting the behavior of fuel rods and fission gases under certain hypothetical light-water-reactor (LWR) accident conditions. To satisfy this need, a comprehensive computer-base model, the Steady-state and Transient Gas-release and Swelling Subroutine (GRASS-SST), its faster-running version, FASTGRASS, and correlations based on analyses performed with GRASS-SST, PARAGRASS, are being developed at Argonne National Laboratory (ANL). This model is being incorporated into the Fuel-rod Analysis Program (FRAP) code being developed by EG&G Idaho, Inc., at the Idaho National Engineering Laboratory (INEL).

The analytical effort is supported by a data base and correlations developed from characterization of irradiated LWR fuel and from out-of-reactor transient heating tests of irradiated commercial and experimental LWR fuel under a range of thermal conditions.

B. Modeling of Fuel/Fission-product Behavior (K. R. Greene and J. Rest, MSD)

1. PARAGRASS Development

a. Introduction

Work was initiated this quarter on the development of PARAGRASS, a parametric model for steady-state and transient fission-gas release and swelling. PARAGRASS is being developed from a data base generated from GRASS-SST[1] and FASTGRASS calculations and will provide the user with an additional option for the calculation of the response of fission gas. PARAGRASS is primarily being designed for situations in which maximal execution efficiency is required.

The initial effort on PARAGRASS development has focused on a scoping-type study in order to best identify the appropriate developmental methodology. Although the initial analysis is for steady-state conditions, it will ultimately include transient phenomena.

b. GRASS-SST Data-base Generation for Steady-state Conditions

Many factors affect the behavior of fission gas. For this initial analysis, four independent variables are considered: burnup, temperature, temperature gradient, and grain size. Table I lists the initial choice of independent variables and their range of values for the GRASS-SST steady-state data-base generation. Table II lists some variables that affect fission-gas behavior.

TABLE I. Independent Parameter Values Used in GRASS-SST Data-base Generation

Burnup, at. %	Temperature, K	Temperature Gradient, °C/cm	Grain Size, microns
0.5-5.0	1100-2300	1000-3000	5-30

TABLE II. Some Variables Affecting Fission-gas Behavior

Temperature
Temperature Gradient
Matrix Stress
Matrix-stress Gradient
Fission Rate
Irradiation Time or Burnup
Fuel Properties:
Density
Vapor pressure
Surface tension
Coefficients of thermal surface and bulk diffusion
Creep Strength
Fission-gas Properties:
Nuclear yields
Equation of state
Diffusion coefficient in the solid fuel
Diffusion coefficient of the gaseous fuel
Fuel Microstructure:
Dislocation density
Grain size
Restructuring
Microcracking

Table III lists the values of various "fixed" parameters, which complete the description of the hypothetical fuel element used for the GRASS-SST data-base generation. For this study the average hydrostatic pressure in the fuel was taken to be equal to the plenum pressure.

TABLE III. Fuel-Element Description

Radius of Element	0.471 cm
Height of Element	1.0 cm
Fuel Density	10.15 g/cm^3
Linear Power Density	10 kW/ft (32.8 kW/m)
Fuel-porosity Fraction	0.07475
Radial Flux-depression Factor	1.0
Total Amount of Fill Gas in Gap and Plenum	0
Plenum Pressure	500 psi (3.45 MPa)

Table IV shows the results of the 560 GRASS-SST runs required to complete the analysis described in Table I. As the number of independent variables is increased and/or the range of the variables is broadened, the number of runs required to define the data base will grow as

$$A_i B_j C_k \ldots Z_l,$$

where A_i is the number of values of the independent variable A, and so on. Thus, the utilization of physical insight for the selection of the parameter values and their associated ranges is essential in order to keep the problem within a reasonable degree of complexity. Note that only gas release (GASOUT) has been chosen as a dependent variable. Other possible dependent variables are:

(1) Average bubble size.

(2) Fraction of retained gas in lattice, on grain boundaries, and along grain edges.

(3) Fission-gas-bubble induced swelling.

Figure 1 shows GRASS-SST-calculated fractional fission-gas release versus burnup and temperature for 10-μm-size grains. In general, fractional gas release is seen to increase with both temperature and burnup. The prediction of higher fractional gas release at 1700 K than at 2000 K at 5 at. % burnup is most likely due to the decreased mobility of the larger intragranular bubbles at 2000 K than at 1700 K in the relatively mild 2000°C/cm temperature gradient.

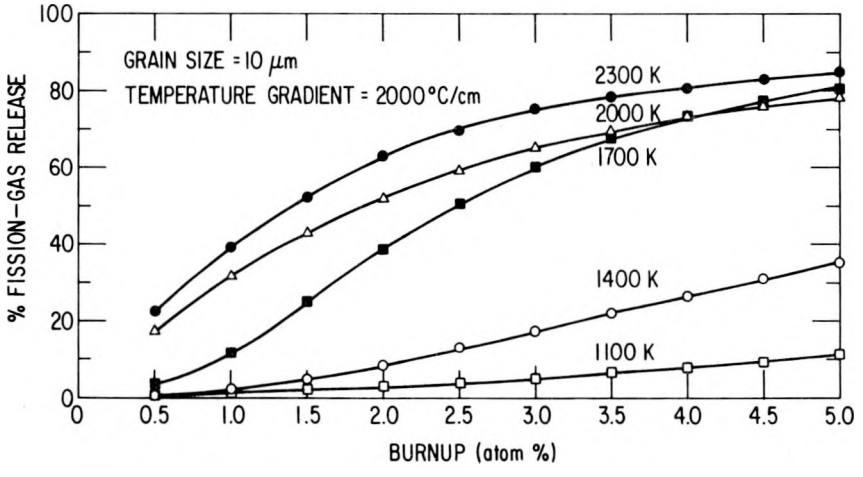

Fig. 1. GRASS-SST-calculated Fractional Fission-gas Release vs Burnup and Temperature

TABLE IV. Results of GRASS-SST Data-base Generation

OBS	TEMPAVG	GRADIENT	GRSIZE	BURNUP	GASOUT	OBS	TEMPAVG	GRADIENT	GRSIZE	BURNUP	GASOUT
1	2300	-2000	30	0.5	36.67	57	2300	-1000	20	3.5	84.84
2	2300	-2000	30	1.0	57.64	58	2300	-1000	20	4.0	87.22
3	2300	-2000	30	1.5	70.04	59	2300	-1000	20	4.5	88.88
4	2300	-2000	30	2.0	77.48	60	2300	-1000	20	5.0	90.53
5	2300	-2000	30	2.5	82.15	61	2300	-1000	10	0.5	23.88
6	2300	-2000	30	3.0	84.21	62	2300	-1000	10	1.0	42.20
7	2300	-2000	30	3.5	86.29	63	2300	-1000	10	1.5	54.88
8	2300	-2000	30	4.0	88.33	64	2300	-1000	10	2.0	65.38
9	2300	-2000	30	4.5	89.26	65	2300	-1000	10	2.5	71.07
10	2300	-2000	30	5.0	91.62	66	2300	-1000	10	3.0	75.84
11	2300	-2000	20	0.5	28.88	67	2300	-1000	10	3.5	79.51
12	2300	-2000	20	1.0	49.36	68	2300	-1000	10	4.0	82.03
13	2300	-2000	20	1.5	63.75	69	2300	-1000	10	4.5	83.92
14	2300	-2000	20	2.0	72.69	70	2300	-1000	10	5.0	84.78
15	2300	-2000	20	2.5	77.48	71	2300	-1000	5	0.5	18.39
16	2300	-2000	20	3.0	81.22	72	2300	-1000	5	1.0	33.17
17	2300	-2000	20	3.5	83.68	73	2300	-1000	5	1.5	44.88
18	2300	-2000	20	4.0	85.51	74	2300	-1000	5	2.0	53.72
19	2300	-2000	20	4.5	87.30	75	2300	-1000	5	2.5	60.91
20	2300	-2000	20	5.0	87.89	76	2300	-1000	5	3.0	66.81
21	2300	-2000	10	0.5	22.73	77	2300	-1000	5	3.5	71.52
22	2300	-2000	10	1.0	38.99	78	2300	-1000	5	4.0	75.21
23	2300	-2000	10	1.5	52.17	79	2300	-1000	5	4.5	77.58
24	2300	-2000	10	2.0	63.03	80	2300	-1000	5	5.0	79.78
25	2300	-2000	10	2.5	69.75	81	2000	-3000	30	0.5	34.62
26	2300	-2000	10	3.0	75.05	82	2000	-3000	30	1.0	56.77
27	2300	-2000	10	3.5	78.54	83	2000	-3000	30	1.5	70.32
28	2300	-2000	10	4.0	80.58	84	2000	-3000	30	2.0	77.16
29	2300	-2000	10	4.5	83.03	85	2000	-3000	30	2.5	82.82
30	2300	-2000	10	5.0	84.77	86	2000	-3000	30	3.0	85.77
31	2300	-2000	5	0.5	17.73	87	2000	-3000	30	3.5	87.25
32	2300	-2000	5	1.0	30.96	88	2000	-3000	30	4.0	89.01
33	2300	-2000	5	1.5	41.85	89	2000	-3000	30	4.5	89.63
34	2300	-2000	5	2.0	52.02	90	2000	-3000	30	5.0	90.95
35	2300	-2000	5	2.5	53.68	91	2000	-3000	20	0.5	21.97
36	2300	-2000	5	3.0	65.76	92	2000	-3000	20	1.0	40.89
37	2300	-2000	5	3.5	70.07	93	2000	-3000	20	1.5	52.95
38	2300	-2000	5	4.0	73.46	94	2000	-3000	20	2.0	62.51
39	2300	-2000	5	4.5	76.46	95	2000	-3000	20	2.5	69.46
40	2300	-2000	5	5.0	78.80	96	2000	-3000	20	3.0	75.28
41	2300	-1000	30	0.5	34.62	97	2000	-3000	20	3.5	79.20
42	2300	-1000	30	1.0	57.89	98	2000	-3000	20	4.0	81.65
43	2300	-1000	30	1.5	70.58	99	2000	-3000	20	4.5	83.12
44	2300	-1000	30	2.0	77.74	100	2000	-3000	20	5.0	85.09
45	2300	-1000	30	2.5	82.19	101	2000	-3000	10	0.5	16.36
46	2300	-1000	30	3.0	85.77	102	2000	-3000	10	1.0	30.58
47	2300	-1000	30	3.5	86.38	103	2000	-3000	10	1.5	41.08
48	2300	-1000	30	4.0	87.25	104	2000	-3000	10	2.0	50.33
49	2300	-1000	30	4.5	88.69	105	2000	-3000	10	2.5	57.83
50	2300	-1000	30	5.0	90.65	106	2000	-3000	10	3.0	63.75
51	2300	-1000	20	0.5	31.43	107	2000	-3000	10	3.5	68.38
52	2300	-1000	20	1.0	50.78	108	2000	-3000	10	4.0	71.94
53	2300	-1000	20	1.5	64.15	109	2000	-3000	10	4.5	74.92
54	2300	-1000	20	2.0	72.45	110	2000	-3000	10	5.0	77.27
55	2300	-1000	20	2.5	78.64	111	2000	-3000	5	0.5	11.58
56	2300	-1000	20	3.0	80.77	112	2000	-3000	5	1.0	20.65

TABLE IV (Contd.)

OBS	TEMPAVG	GRADIENT	GRSIZE	BURNUP	GASOUT	OBS	TEMPAVG	GRADIENT	GRSIZE	BURNUP	GASOUT
113	2000	-3000	5	1.5	29.59	169	2000	-1000	30	4.5	90.720
114	2000	-3000	5	2.0	37.30	170	2000	-1000	30	5.0	91.560
115	2000	-3000	5	2.5	43.70	171	2000	-1000	20	0.5	31.720
116	2000	-3000	5	3.0	49.33	172	2000	-1000	20	1.0	51.020
117	2000	-3000	5	3.5	54.25	173	2000	-1000	20	1.5	64.810
118	2000	-3000	5	4.0	58.48	174	2000	-1000	20	2.0	72.650
119	2000	-3000	5	4.5	62.11	175	2000	-1000	20	2.5	77.570
120	2000	-3000	5	5.0	65.24	176	2000	-1000	20	3.0	81.250
121	2000	-2000	30	0.5	33.76	177	2000	-1000	20	3.5	84.340
122	2000	-2000	30	1.0	56.62	178	2000	-1000	20	4.0	86.760
123	2000	-2000	30	1.5	68.73	179	2000	-1000	20	4.5	87.430
124	2000	-2000	30	2.0	76.02	180	2000	-1000	20	5.0	88.960
125	2000	-2000	30	2.5	80.47	181	2000	-1000	10	0.5	18.090
126	2000	-2000	30	3.0	83.65	182	2000	-1000	10	1.0	33.370
127	2000	-2000	30	3.5	85.83	183	2000	-1000	10	1.5	44.870
128	2000	-2000	30	4.0	87.75	184	2000	-1000	10	2.0	53.810
129	2000	-2000	30	4.5	89.04	185	2000	-1000	10	2.5	60.940
130	2000	-2000	30	5.0	90.09	186	2000	-1000	10	3.0	66.390
131	2000	-2000	20	0.5	23.36	187	2000	-1000	10	3.5	70.630
132	2000	-2000	20	1.0	43.22	188	2000	-1000	10	4.0	73.990
133	2000	-2000	20	1.5	55.83	189	2000	-1000	10	4.5	76.700
134	2000	-2000	20	2.0	65.76	190	2000	-1000	10	5.0	78.930
135	2000	-2000	20	2.5	73.29	191	2000	-1000	5	0.5	14.640
136	2000	-2000	20	3.0	78.00	192	2000	-1000	5	1.0	26.890
137	2000	-2000	20	3.5	80.98	193	2000	-1000	5	1.5	36.960
138	2000	-2000	20	4.0	83.48	194	2000	-1000	5	2.0	45.030
139	2000	-2000	20	4.5	85.61	195	2000	-1000	5	2.5	52.480
140	2000	-2000	20	5.0	86.70	196	2000	-1000	5	3.0	58.170
141	2000	-2000	10	0.5	17.39	197	2000	-1000	5	3.5	63.230
142	2000	-2000	10	1.0	31.57	198	2000	-1000	5	4.0	67.000
143	2000	-2000	10	1.5	42.96	199	2000	-1000	5	4.5	70.230
144	2000	-2000	10	2.0	51.78	200	2000	-1000	5	5.0	73.000
145	2000	-2000	10	2.5	59.10	201	1700	-3000	30	0.5	0.972
146	2000	-2000	10	3.0	64.91	202	1700	-3000	30	1.0	4.466
147	2000	-2000	10	3.5	69.45	203	1700	-3000	30	1.5	13.360
148	2000	-2000	10	4.0	73.20	204	1700	-3000	30	2.0	30.760
149	2000	-2000	10	4.5	75.91	205	1700	-3000	30	2.5	43.360
150	2000	-2000	10	5.0	78.26	206	1700	-3000	30	3.0	51.200
151	2000	-2000	5	0.5	12.92	207	1700	-3000	30	3.5	57.520
152	2000	-2000	5	1.0	22.60	208	1700	-3000	30	4.0	62.460
153	2000	-2000	5	1.5	32.07	209	1700	-3000	30	4.5	66.370
154	2000	-2000	5	2.0	40.51	210	1700	-3000	30	5.0	69.640
155	2000	-2000	5	2.5	47.47	211	1700	-3000	20	0.5	1.626
156	2000	-2000	5	3.0	54.01	212	1700	-3000	20	1.0	6.908
157	2000	-2000	5	3.5	59.46	213	1700	-3000	20	1.5	17.520
158	2000	-2000	5	4.0	63.74	214	1700	-3000	20	2.0	31.560
159	2000	-2000	5	4.5	67.19	215	1700	-3000	20	2.5	47.290
160	2000	-2000	5	5.0	70.74	216	1700	-3000	20	3.0	57.510
161	2000	-1000	30	0.5	40.47	217	1700	-3000	20	3.5	64.180
162	2000	-1000	30	1.0	62.92	218	1700	-3000	20	4.0	69.130
163	2000	-1000	30	1.5	73.60	219	1700	-3000	20	4.5	72.990
164	2000	-1000	30	2.0	79.93	220	1700	-3000	20	5.0	76.050
165	2000	-1000	30	2.5	83.75	221	1700	-3000	10	0.5	3.322
166	2000	-1000	30	3.0	86.37	222	1700	-3000	10	1.0	10.100
167	2000	-1000	30	3.5	88.25	223	1700	-3000	10	1.5	21.580
168	2000	-1000	30	4.0	89.58	224	1700	-3000	10	2.0	33.790

TABLE IV (Contd.)

OBS	TEMPAVG	GRADIENT	GRSIZE	BURNUP	GASOUT	OBS	TEMPAVG	GRADIENT	GRSIZE	BURNUP	GASOUT
225	1700	-3000	10	2.5	44.680	281	1700	-1000	30	0.5	0.790
226	1700	-3000	10	3.0	54.240	282	1700	-1000	30	1.0	4.777
227	1700	-3000	10	3.5	61.790	283	1700	-1000	30	1.5	11.950
228	1700	-3000	10	4.0	67.690	284	1700	-1000	30	2.0	19.440
229	1700	-3000	10	4.5	72.300	285	1700	-1000	30	2.5	26.310
230	1700	-3000	10	5.0	75.930	286	1700	-1000	30	3.0	32.150
231	1700	-3000	5	0.5	5.828	287	1700	-1000	30	3.5	37.250
232	1700	-3000	5	1.0	13.440	288	1700	-1000	30	4.0	42.040
233	1700	-3000	5	1.5	22.520	289	1700	-1000	30	4.5	46.880
234	1700	-3000	5	2.0	30.860	290	1700	-1000	30	5.0	51.470
235	1700	-3000	5	2.5	37.840	291	1700	-1000	20	0.5	1.423
236	1700	-3000	5	3.0	43.590	292	1700	-1000	20	1.0	7.883
237	1700	-3000	5	3.5	48.510	293	1700	-1000	20	1.5	18.760
238	1700	-3000	5	4.0	53.090	294	1700	-1000	20	2.0	29.580
239	1700	-3000	5	4.5	57.030	295	1700	-1000	20	2.5	38.490
240	1700	-3000	5	5.0	60.550	296	1700	-1000	20	3.0	45.650
241	1700	-2000	30	0.5	0.881	297	1700	-1000	20	3.5	51.520
242	1700	-2000	30	1.0	4.551	298	1700	-1000	20	4.0	56.460
243	1700	-2000	30	1.5	12.270	299	1700	-1000	20	4.5	60.690
244	1700	-2000	30	2.0	20.680	300	1700	-1000	20	5.0	64.390
245	1700	-2000	30	2.5	29.020	301	1700	-1000	10	0.5	3.727
246	1700	-2000	30	3.0	37.590	302	1700	-1000	10	1.0	14.660
247	1700	-2000	30	3.5	45.320	303	1700	-1000	10	1.5	30.550
248	1700	-2000	30	4.0	51.330	304	1700	-1000	10	2.0	45.600
249	1700	-2000	30	4.5	56.070	305	1700	-1000	10	2.5	57.670
250	1700	-2000	30	5.0	59.690	306	1700	-1000	10	3.0	66.500
251	1700	-2000	20	0.5	1.611	307	1700	-1000	10	3.5	72.980
252	1700	-2000	20	1.0	7.126	308	1700	-1000	10	4.0	77.820
253	1700	-2000	20	1.5	17.920	309	1700	-1000	10	4.5	81.490
254	1700	-2000	20	2.0	29.410	310	1700	-1000	10	5.0	84.320
255	1700	-2000	20	2.5	39.430	311	1700	-1000	5	0.5	6.795
256	1700	-2000	20	3.0	47.460	312	1700	-1000	5	1.0	18.320
257	1700	-2000	20	3.5	54.140	313	1700	-1000	5	1.5	31.210
258	1700	-2000	20	4.0	59.830	314	1700	-1000	5	2.0	41.590
259	1700	-2000	20	4.5	64.630	315	1700	-1000	5	2.5	49.540
260	1700	-2000	20	5.0	68.740	316	1700	-1000	5	3.0	56.250
261	1700	-2000	10	0.5	3.486	317	1700	-1000	5	3.5	61.590
262	1700	-2000	10	1.0	11.710	318	1700	-1000	5	4.0	65.890
263	1700	-2000	10	1.5	25.130	319	1700	-1000	5	4.5	69.420
264	1700	-2000	10	2.0	38.400	320	1700	-1000	5	5.0	72.340
265	1700	-2000	10	2.5	50.560	321	1400	-3000	30	0.5	0.126
266	1700	-2000	10	3.0	60.100	322	1400	-3000	30	1.0	0.534
267	1700	-2000	10	3.5	67.390	323	1400	-3000	30	1.5	0.953
268	1700	-2000	10	4.0	72.940	324	1400	-3000	30	2.0	1.515
269	1700	-2000	10	4.5	77.190	325	1400	-3000	30	2.5	2.254
270	1700	-2000	10	5.0	80.480	326	1400	-3000	30	3.0	3.174
271	1700	-2000	5	0.5	6.034	327	1400	-3000	30	3.5	4.257
272	1700	-2000	5	1.0	14.760	328	1400	-3000	30	4.0	5.464
273	1700	-2000	5	1.5	25.060	329	1400	-3000	30	4.5	6.753
274	1700	-2000	5	2.0	34.160	330	1400	-3000	30	5.0	8.039
275	1700	-2000	5	2.5	41.470	331	1400	-3000	20	0.5	0.284
276	1700	-2000	5	3.0	47.330	332	1400	-3000	20	1.0	0.890
277	1700	-2000	5	3.5	52.700	333	1400	-3000	20	1.5	1.739
278	1700	-2000	5	4.0	57.300	334	1400	-3000	20	2.0	2.952
279	1700	-2000	5	4.5	61.210	335	1400	-3000	20	2.5	4.542
280	1700	-2000	5	5.0	64.560	336	1400	-3000	20	3.0	6.440

TABLE IV (Contd.)

OBS	TEMPAVG	GRADIENT	GRSIZE	BURNUP	GASOUT	OBS	TEMPAVG	GRADIENT	GRSIZE	BURNUP	GASOUT
337	1400	-3000	20	3.5	8.538	393	1400	-2000	5	1.5	13.350
338	1400	-3000	20	4.0	10.740	394	1400	-2000	5	2.0	22.270
339	1400	-3000	20	4.5	12.950	395	1400	-2000	5	2.5	30.670
340	1400	-3000	20	5.0	15.140	396	1400	-2000	5	3.0	38.290
341	1400	-3000	10	0.5	0.583	397	1400	-2000	5	3.5	45.370
342	1400	-3000	10	1.0	2.277	398	1400	-2000	5	4.0	51.410
343	1400	-3000	10	1.5	5.201	399	1400	-2000	5	4.5	56.520
344	1400	-3000	10	2.0	9.287	400	1400	-2000	5	5.0	60.850
345	1400	-3000	10	2.5	13.930	401	1400	-1000	30	0.5	0.183
346	1400	-3000	10	3.0	18.790	402	1400	-1000	30	1.0	0.513
347	1400	-3000	10	3.5	23.420	403	1400	-1000	30	1.5	0.871
348	1400	-3000	10	4.0	28.000	404	1400	-1000	30	2.0	1.330
349	1400	-3000	10	4.5	32.500	405	1400	-1000	30	2.5	1.921
350	1400	-3000	10	5.0	36.650	406	1400	-1000	30	3.0	2.658
351	1400	-3000	5	0.5	1.227	407	1400	-1000	30	3.5	3.540
352	1400	-3000	5	1.0	5.900	408	1400	-1000	30	4.0	4.548
353	1400	-3000	5	1.5	14.180	409	1400	-1000	30	4.5	5.656
354	1400	-3000	5	2.0	23.540	410	1400	-1000	30	5.0	6.836
355	1400	-3000	5	2.5	32.160	411	1400	-1000	20	0.5	0.287
356	1400	-3000	5	3.0	40.140	412	1400	-1000	20	1.0	0.840
357	1400	-3000	5	3.5	47.260	413	1400	-1000	20	1.5	1.546
358	1400	-3000	5	4.0	53.260	414	1400	-1000	20	2.0	2.519
359	1400	-3000	5	4.5	58.290	415	1400	-1000	20	2.5	3.799
360	1400	-3000	5	5.0	62.540	416	1400	-1000	20	3.0	5.367
361	1400	-2000	30	0.5	0.187	417	1400	-1000	20	3.5	7.161
362	1400	-2000	30	1.0	0.524	418	1400	-1000	20	4.0	9.107
363	1400	-2000	30	1.5	0.914	419	1400	-1000	20	4.5	11.130
364	1400	-2000	30	2.0	1.426	420	1400	-1000	20	5.0	13.170
365	1400	-2000	30	2.5	2.094	421	1400	-1000	10	0.5	0.586
366	1400	-2000	30	3.0	2.928	422	1400	-1000	10	1.0	2.078
367	1400	-2000	30	3.5	3.918	423	1400	-1000	10	1.5	4.459
368	1400	-2000	30	4.0	5.034	424	1400	-1000	10	2.0	7.831
369	1400	-2000	30	4.5	6.242	425	1400	-1000	10	2.5	11.900
370	1400	-2000	30	5.0	7.510	426	1400	-1000	10	3.0	16.250
371	1400	-2000	20	0.5	0.285	427	1400	-1000	10	3.5	20.610
372	1400	-2000	20	1.0	0.867	428	1400	-1000	10	4.0	24.800
373	1400	-2000	20	1.5	1.647	429	1400	-1000	10	4.5	28.970
374	1400	-2000	20	2.0	2.746	430	1400	-1000	10	5.0	33.080
375	1400	-2000	20	2.5	4.191	431	1400	-1000	5	0.5	1.180
376	1400	-2000	20	3.0	5.938	432	1400	-1000	5	1.0	5.295
377	1400	-2000	20	3.5	7.901	433	1400	-1000	5	1.5	12.300
378	1400	-2000	20	4.0	9.990	434	1400	-1000	5	2.0	20.640
379	1400	-2000	20	4.5	12.130	435	1400	-1000	5	2.5	28.720
380	1400	-2000	20	5.0	14.250	436	1400	-1000	5	3.0	36.020
381	1400	-2000	10	0.5	0.583	437	1400	-1000	5	3.5	42.970
382	1400	-2000	10	1.0	2.187	438	1400	-1000	5	4.0	49.020
383	1400	-2000	10	1.5	4.853	439	1400	-1000	5	4.5	54.200
384	1400	-2000	10	2.0	8.619	440	1400	-1000	5	5.0	58.640
385	1400	-2000	10	2.5	13.040	441	1100	-3000	30	0.5	0.228
386	1400	-2000	10	3.0	17.650	442	1100	-3000	30	1.0	0.429
387	1400	-2000	10	3.5	22.170	443	1100	-3000	30	1.5	0.595
388	1400	-2000	10	4.0	26.530	444	1100	-3000	30	2.0	0.757
389	1400	-2000	10	4.5	30.960	445	1100	-3000	30	2.5	0.929
390	1400	-2000	10	5.0	35.100	446	1100	-3000	30	3.0	1.116
391	1400	-2000	5	0.5	1.204	447	1100	-3000	30	3.5	1.323
392	1400	-2000	5	1.0	5.634	448	1100	-3000	30	4.0	1.553

TABLE IV (Contd.)

OBS	TEMPAVG	GRADIENT	GRSIZE	BURNUP	GASOUT	OBS	TEMPAVG	GRADIENT	GRSIZE	BURNUP	GASOUT
449	1100	-3000	30	4.5	1.810	505	1100	-2000	10	2.5	3.874
450	1100	-3000	30	5.0	2.094	506	1100	-2000	10	3.0	5.052
451	1100	-3000	20	0.5	0.354	507	1100	-2000	10	3.5	6.423
452	1100	-3000	20	1.0	0.663	508	1100	-2000	10	4.0	7.975
453	1100	-3000	20	1.5	0.937	509	1100	-2000	10	4.5	9.687
454	1100	-3000	20	2.0	1.226	510	1100	-2000	10	5.0	11.530
455	1100	-3000	20	2.5	1.547	511	1100	-2000	5	0.5	1.162
456	1100	-3000	20	3.0	1.914	512	1100	-2000	5	1.0	2.710
457	1100	-3000	20	3.5	2.333	513	1100	-2000	5	1.5	4.476
458	1100	-3000	20	4.0	2.810	514	1100	-2000	5	2.0	6.653
459	1100	-3000	20	4.5	3.349	515	1100	-2000	5	2.5	9.242
460	1100	-3000	20	5.0	3.951	516	1100	-2000	5	3.0	12.170
461	1100	-3000	10	0.5	0.670	517	1100	-2000	5	3.5	15.300
462	1100	-3000	10	1.0	1.362	518	1100	-2000	5	4.0	18.530
463	1100	-3000	10	1.5	2.064	519	1100	-2000	5	4.5	21.750
464	1100	-3000	10	2.0	2.836	520	1100	-2000	5	5.0	24.880
465	1100	-3000	10	2.5	3.875	521	1100	-1000	30	0.5	0.228
466	1100	-3000	10	3.0	5.053	522	1100	-1000	30	1.0	0.429
467	1100	-3000	10	3.5	6.424	523	1100	-1000	30	1.5	0.594
468	1100	-3000	10	4.0	7.977	524	1100	-1000	30	2.0	0.757
469	1100	-3000	10	4.5	9.689	525	1100	-1000	30	2.5	0.928
470	1100	-3000	10	5.0	11.530	526	1100	-1000	30	3.0	1.116
471	1100	-3000	5	0.5	1.162	527	1100	-1000	30	3.5	1.323
472	1100	-3000	5	1.0	2.711	528	1100	-1000	30	4.0	1.552
473	1100	-3000	5	1.5	4.478	529	1100	-1000	30	4.5	1.809
474	1100	-3000	5	2.0	6.655	530	1100	-1000	30	5.0	2.093
475	1100	-3000	5	2.5	9.245	531	1100	-1000	20	0.5	0.354
476	1100	-3000	5	3.0	12.170	532	1100	-1000	20	1.0	0.662
477	1100	-3000	5	3.5	15.310	533	1100	-1000	20	1.5	0.937
478	1100	-3000	5	4.0	18.540	534	1100	-1000	20	2.0	1.225
479	1100	-3000	5	4.5	21.750	535	1100	-1000	20	2.5	1.547
480	1100	-3000	5	5.0	24.890	536	1100	-1000	20	3.0	1.913
481	1100	-2000	30	0.5	0.228	537	1100	-1000	20	3.5	2.332
482	1100	-2000	30	1.0	0.429	538	1100	-1000	20	4.0	2.809
483	1100	-2000	30	1.5	0.594	539	1100	-1000	20	4.5	3.347
484	1100	-2000	30	2.0	0.757	540	1100	-1000	20	5.0	3.950
485	1100	-2000	30	2.5	0.929	541	1100	-1000	10	0.5	0.669
486	1100	-2000	30	3.0	1.116	542	1100	-1000	10	1.0	1.361
487	1100	-2000	30	3.5	1.323	543	1100	-1000	10	1.5	2.063
488	1100	-2000	30	4.0	1.553	544	1100	-1000	10	2.0	2.835
489	1100	-2000	30	4.5	1.809	545	1100	-1000	10	2.5	3.873
490	1100	-2000	30	5.0	2.093	546	1100	-1000	10	3.0	5.050
491	1100	-2000	20	0.5	0.354	547	1100	-1000	10	3.5	6.420
492	1100	-2000	20	1.0	0.663	548	1100	-1000	10	4.0	7.973
493	1100	-2000	20	1.5	0.937	549	1100	-1000	10	4.5	9.684
494	1100	-2000	20	2.0	1.225	550	1100	-1000	10	5.0	11.520
495	1100	-2000	20	2.5	1.547	551	1100	-1000	5	0.5	1.161
496	1100	-2000	20	3.0	1.913	552	1100	-1000	5	1.0	2.709
497	1100	-2000	20	3.5	2.332	553	1100	-1000	5	1.5	4.475
498	1100	-2000	20	4.0	2.809	554	1100	-1000	5	2.0	6.651
499	1100	-2000	20	4.5	3.348	555	1100	-1000	5	2.5	9.239
500	1100	-2000	20	5.0	3.951	556	1100	-1000	5	3.0	12.160
501	1100	-2000	10	0.5	0.670	557	1100	-1000	5	3.5	15.300
502	1100	-2000	10	1.0	1.362	558	1100	-1000	5	4.0	18.530
503	1100	-2000	10	1.5	2.063	559	1100	-1000	5	4.5	21.740
504	1100	-2000	10	2.0	2.885	560	1100	-1000	5	5.0	24.880

Figure 2 shows GRASS-SST-calculated fractional fission-gas release versus burnup and grain size for a 2000 K temperature and 2000°C/cm temperature gradient. An interesting peculiarity is evident in Fig. 2, where the predicted fractional fission-gas release increases with increasing grain size. These results should be compared to those of Fig. 3, which show the gas-release predictions as a function of grain size and burnup at the lower 1100 K temperature. The results shown in Fig. 3 follow conventional expectations in that gas release increases with decreasing grain size. The overall GRASS-SST-predicted dependence of gas release on grain size and temperature is shown in Fig. 4. As seen in Fig. 4, the transition temperature at which the dependence of gas release on grain size reverses is predicted to be between 1500 and 1700 K. The reason for this apparent anomaly is as follows:

In all cases, the GRASS-SST-predicted intragranular gas release increases as the grain size decreases.[1] However, as the grain size increases, the grain-boundary area per unit volume decreases, so that for a given amount of intergranular fission gas, the amount of intergranular gas per unit area of grain boundary increases as the grain size increases. The increase in the intergranular bubble density results in increased bubble coalescence and larger bubbles on the grain boundaries. The current version of the GRASS-SST code does not include a calculation of the grain-edge bubble density (only bulk, dislocation, and grain-face bubble distributions are calculated), but instead uses the assumption that the predicted grain-edge swelling is directly dependent on the calculation of the average grain-face bubble size. On the other hand, the edge-tunnel interlinkage probability is directly dependent on the grain-edge swelling. Thus, at relatively high temperatures, where the fraction of retained gas on the boundaries is sufficiently high, the dependence of the edge-tunnel interlinkage probability on grain size (interlinkage increases as grain size increases) dominates over the dependence of intragranular gas release on grain size (intragranular gas release decreases as grain size increases). Thus, the predicted fractional gas release increases as grain size increases.

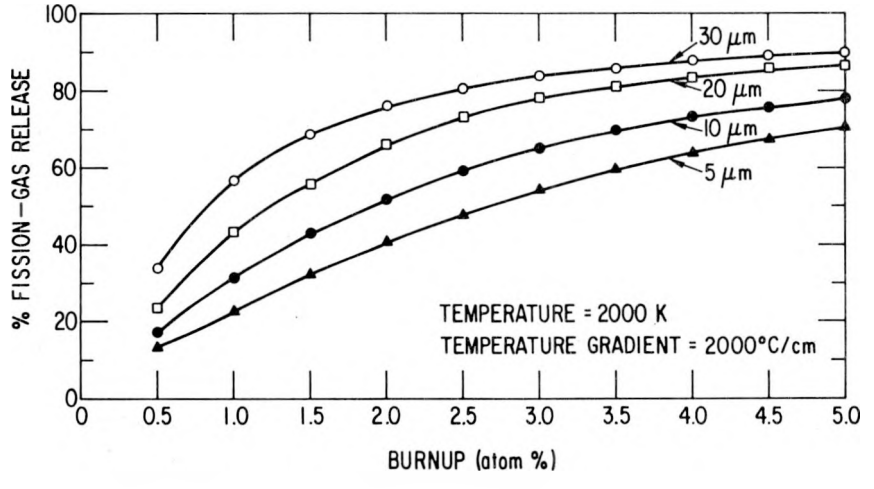

Fig. 2

GRASS-SST-calculated Fractional Fission-gas Release vs Burnup and Grain Size for a Fuel Temperature of 2000 K

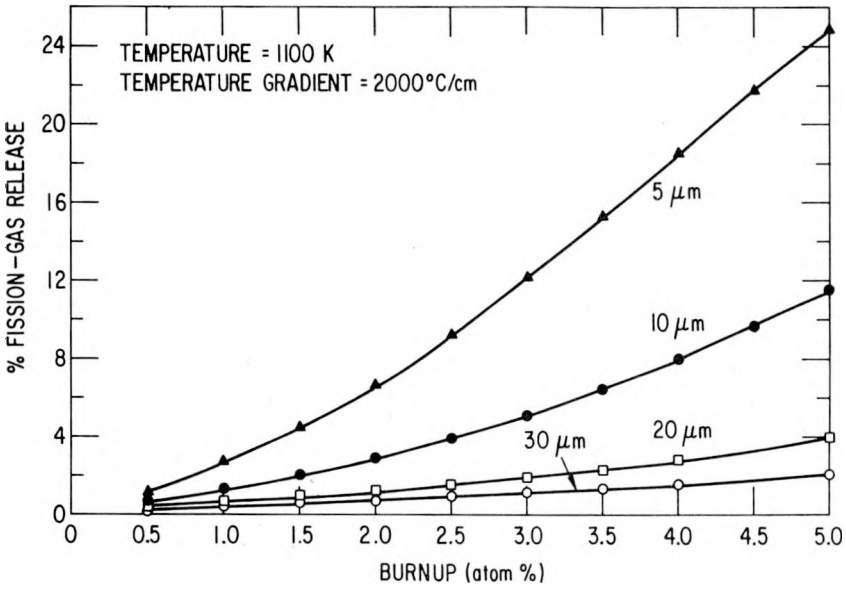

Fig. 3

GRASS-SST-calculated Fractional Fission-gas Release vs Burnup and Grain Size for a Fuel Temperature of 1100 K

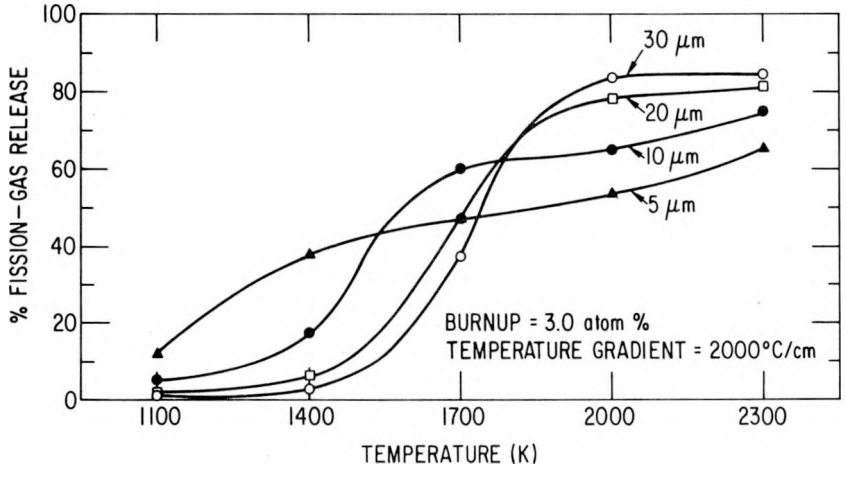

Fig. 4. GRASS-SST-calculated Fractional Fission-gas Release vs Temperature and Grain Size

FASTGRASS does not use the above-mentioned assumption governing the mechanics of edge-tunnel interlinkage, but instead directly calculates the evolution of an average-size grain-edge bubble. In addition, FASTGRASS-predicted gas release decreases as the grain size increases for both low- and high-temperature environments. Thus, the above assumption used in GRASS-SST is suspect. GRASS-SST is currently being modified to include a calculation for the evolution of an average-size grain-edge bubble. This new version of GRASS-SST, which will be completed shortly, will be checked out and used in future PARAGRASS developmental analyses.

Figures 5-7 show GRASS-SST-calculated fractional fission-gas release versus burnup and temperature gradient, temperature and temperature gradient, and grain size and temperature gradient, respectively. In general,

the predicted dependence of gas release on temperature gradient is relatively weak. However, the predicted trend is that gas release decreases with increasing temperature gradient. Again, this goes against conventional intuition. The reason for this trend can be traced to the above-mentioned assumption governing the mechanics of edge-tunnel interlinkage. In a relatively high temperature gradient, the residence time of bubbles on the grain faces is shorter, and thus the average bubble size is smaller than what it would be in a lower gradient. The smaller average-size bubble results in lower grain-edge swelling, and thus in less grain-edge tunnel interlinkage: hence, less gas release with increased temperature gradient. This phenomenon is expected to disappear when the new version of GRASS-SST is implemented.

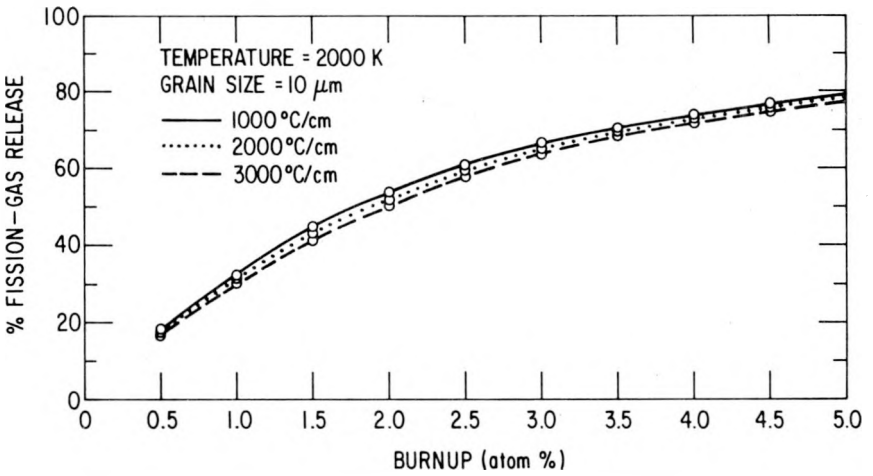

Fig. 5. GRASS-SST-calculated Fractional Fission-gas Release vs Burnup and Temperature Gradient

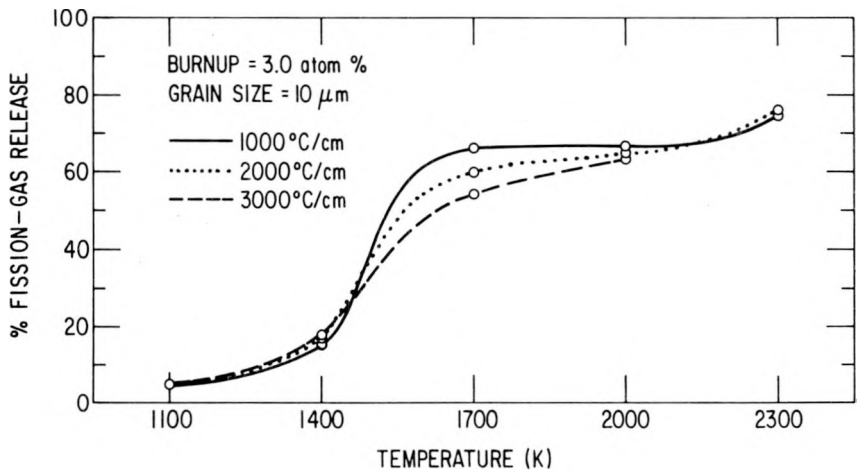

Fig. 6. GRASS-SST-calculated Fractional Fission-gas Release vs Temperature and Temperature Gradient

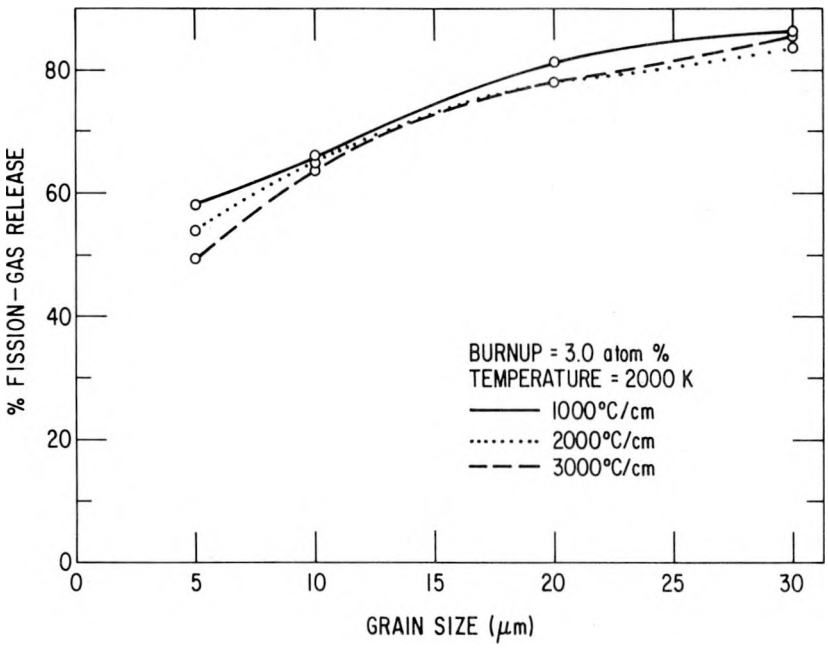

Fig. 7

GRASS-SST-calculated Fractional Fission-gas Release vs Grain Size and Temperature Gradient

c. Data Analysis

A computerized statistical-analysis package[2] was used for the data analysis. The curves were fit with a linear-regression model. The expression for the correlation is polynomial in form with degree 5. Although a polynomial expression does not have any physical significance to fission-gas release, it is an expression that can be made to fit nearly all curves if enough terms are added. Later in the development of the parametric model, physical significance may be included in the correlations through the inclusion of equations containing Arrhenius-type relationships, and so on.

The first efforts in the analysis were directed toward developing a two-parameter fission-gas-release correlation. The fits were very good, with R^2 generally greater than 0.999 and sometimes equal to 1.000. However, on close analysis of the residuals between parametric-model-predicted values of fission-gas release and GRASS-SST values of gas release, it was discovered that the errors in the region of small gas release were large. The correlation is described in Table V, and the relative errors are shown in Table VI.

The problem was solved by examining the correlation variables. Burnup and temperature range over one or two orders of magnitude. The gas-release percentage ranges over three orders of magnitude. To increase the sensitivity of the correlation at lower gas-release fractions, a semilogarithmic fit in gas-release percentage was used. The model is described in Table VII, and the relative errors are shown in Table VIII.

A correlation was then developed for each set of two of the four independent variables. The linear-regression model was a fifth-degree polynomial logarithmic in gas release. In developing these models, we included

all combinations of the two variables in the equation, and those that did not have any correlation with gas release were marked by the statistical-analysis package and subsequently removed. The correlations are described in Tables VII-XIII.

To consider all combinations of the variables that form the fifth-degree polynomial becomes very cumbersome with each additional parameter. Table XIV shows how many variables would need to be considered. The problem is identifying the significant variable combinations for the parametric equation.

TABLE V. First Try at Correlation for Gas Release as a Function of Burnup and Temperature

$$F = Y_o + K_1T + K_2T^2 + K_3T^3 + K_4T^4 + K_5B + K_6BT + K_7BT^2 + K_8BT^3 + K_9BT^4 + K_{10}B^2 + K_{11}B^2T + K_{12}B^2T^2 + K_{13}B^2T^3 + K_{14}B^2T^4 + K_{15}B^3 + K_{16}B^3T + K_{17}B^3T^2 + K_{18}B^3T^3 + K_{19}B^3T^5 + K_{20}B^4 + K_{21}B^4T + K_{22}B^4T^2 + K_{23}B^4T^4 + K_{24}B^5 + K_{25}B^5T + K_{26}B^5T^2 + K_{27}B^5T^5$$

F = % fission gas release

B = burnup in atom %

T = Temperature in °K

$R^2 = 0.999819$

Grainsize = 10 microns

Temperature gradient = -2000°C/cm

$Y_o = -1899.04001114$

$K_1 = 4.85167364$	$K_{10} = 943.78740009$	$K_{19} = -2.2550371 \times 10^{-15}$
$K_2 = -0.00453101$	$K_{11} = -2.40277324$	$K_{20} = 27.38288878$
$K_3 = 1.8358864 \times 10^{-6}$	$K_{12} = 0.00219218$	$K_{21} = -0.0491037$
$K_4 = -2.7249957 \times 10^{-10}$	$K_{13} = -8.4270507 \times 10^{-7}$	$K_{22} = 2.392195 \times 10^{-5}$
$K_5 = 1070.878951$	$K_{14} = 1.1549751 \times 10^{-10}$	$K_{23} = -1.4593979 \times 10^{-12}$
$K_6 = -2.53354995$	$K_{15} = -252.30822532$	$K_{24} = -1.86284656$
$K_7 = 0.00219044$	$K_{16} = 0.56013319$	$K_{25} = 0.00309519$
$K_8 = -8.3247643 \times 10^{-7}$	$K_{17} = -0.00041708$	$K_{26} = -1.323969 \times 10^{-6}$
$K_9 = 1.1941204 \times 10^{-10}$	$K_{18} = 1.0810132 \times 10^{-7}$	$K_{27} = 2.7011877 \times 10^{-17}$

TABLE VI. Relative Errors between Parametric-model-predicted Values and GRASS-SST-predicted Values of Fission-gas Release for the Model Described in Table V

OBS	GRASS-SST	Parametric Model	%Error	OBS	GRASS-SST	Parametric Model	%Error
30	84.77	84.79	0.02	142	31.57	30.65	2.91
29	83.03	82.83	0.24	389	30.96	30.35	1.97
28	80.58	80.90	0.40	388	26.53	26.25	1.06
270	80.48	80.05	0.53	263	25.13	25.42	1.15
27	78.54	78.49	0.06	21	22.73	22.57	0.70
150	78.26	78.39	0.17	387	22.17	22.29	0.54
269	77.19	77.57	0.49	386	17.65	18.01	2.04
149	75.91	76.03	0.16	141	17.39	17.97	3.34
26	75.05	75.00	0.07	385	13.04	13.37	2.53
148	73.20	72.75	0.61	262	11.71	12.90	10.16
268	72.94	73.46	0.71	510	11.53	11.39	1.21
25	69.75	69.87	0.17	509	9.687	9.893	2.13
147	69.45	69.16	0.42	384	8.619	8.692	0.85
267	67.39	67.56	0.25	508	7.975	8.068	1.17
146	64.91	65.02	0.17	507	6.423	6.343	1.25
24	63.03	62.52	0.81	506	5.052	4.913	2.75
266	60.10	59.70	0.67	383	4.858	4.539	6.57
145	59.10	59.67	0.96	505	3.874	3.804	1.81
23	52.17	52.44	0.52	261	3.486	2.732	21.63
144	51.78	52.33	1.06	504	2.885	2.932	1.63
265	50.56	49.82	1.46	382	2.187	1.679	23.23
143	42.96	42.56	0.93	503	2.063	2.169	5.14
22	38.99	39.23	0.62	502	1.362	1.403	3.01
264	38.40	38.16	0.63	501	0.670	0.603	10.00
390	35.10	35.54	1.25	381	0.588	0.984	67.35

TABLE VII. Correlation for Gas Release as a Function of Burnup and Grain Size

$$F = \exp [Y_o + K_1 S + K_2 S^2 + K_3 S^3 + K_4 B + K_5 BS + K_6 BS^2 + K_7 BS^3 + K_8 B^2 + K_9 B^2 S + K_{10} B^2 S^2 + K_{11} B^2 S^3 + K_{12} B^3 + K_{13} B^3 S + K_{14} B^3 S^2 + K_{15} B^3 S^3 + K_{16} B^4 + K_{17} B^4 S + K_{18} B^4 S^2 + K_{19} B^4 S^3 + K_{20} B^5 + K_{21} B^5 S + K_{22} B^5 S^2 + K_{23} B^5 S^4]$$

F = % fission gas release

B = burnup in atom %

S = grainsize in microns

$R^2 = 0.999808$

Temperature = 2000°K

Temperature Gradient = -2000°C/cm

$Y_o = 1.43570891$

$K_1 = 0.05543468$	$K_9 = -0.20675311$	$K_{17} = -0.012033$
$K_2 = -0.00266034$	$K_{10} = 0.00875634$	$K_{18} = 0.00049926$
$K_3 = 6.5558446 \times 10^{-5}$	$K_{11} = -0.00012063$	$K_{19} = -6.855206 \times 10^{-6}$
$K_4 = 1.37636256$	$K_{12} = -0.00371548$	$K_{20} = -0.00020636$
$K_5 = 0.22041597$	$K_{13} = 0.07425931$	$K_{21} = 0.00066237$
$K_6 = -0.00888405$	$K_{14} = -0.00314620$	$K_{22} = -2.0985954 \times 10^{-5}$
$K_7 = 0.00010636$	$K_{15} = 4.4018404 \times 10^{-5}$	$K_{23} = 5.9762824 \times 10^{-9}$
$K_8 = -0.22965015$	$K_{16} = 0.00512523$	

TABLE VIII. Relative Errors between Parametric-model-predicted Values and GRASS-SST-predicted Values of Fission-gas Release for the Model Described in Table IX

OBS	GRASS-SST	Parametric Model	%Error	OBS	GRASS-SST	Parametric Model	%Error
30	84.77	84.90	0.15	142	31.57	31.44	0.41
29	83.03	82.64	0.47	389	30.96	30.93	0.10
28	80.58	80.95	0.46	388	26.53	26.77	0.90
270	80.48	80.91	0.53	263	25.13	24.72	1.63
27	78.54	78.51	0.04	21	22.73	22.78	0.22
150	78.26	78.14	0.15	387	22.17	22.21	0.18
269	77.19	76.53	0.86	386	17.65	17.49	0.91
149	75.91	75.89	0.03	141	17.39	17.39	0
26	75.05	74.91	0.19	385	13.04	12.91	1.00
148	73.20	73.53	0.45	262	11.71	11.81	0.85
268	72.94	72.77	0.23	510	11.53	11.57	0.35
25	69.75	69.86	0.16	509	9.687	9.595	0.95
147	69.45	69.67	0.32	384	8.619	8.665	0.53
267	67.39	67.60	0.31	508	7.975	8.011	0.45
146	64.91	64.54	0.56	507	6.423	6.469	0.72
24	63.03	62.77	0.41	506	5.052	5.041	0.22
266	60.10	60.33	0.38	383	4.858	4.955	2.00
145	59.10	58.68	0.71	505	3.874	3.843	0.80
23	52.17	52.59	0.81	261	3.486	3.485	0.03
144	51.78	51.96	0.35	504	2.885	2.886	0.03
265	50.56	50.69	0.26	382	2.187	2.150	1.69
143	42.96	43.30	0.79	503	2.063	2.087	1.16
22	38.99	38.73	0.67	502	1.362	1.349	0.95
264	38.40	38.58	0.47	501	0.670	0.672	0.30
390	35.10	35.03	0.10	381	0.588	0.590	0.34

TABLE IX. Second Try at Correlation for Gas Release as a Function of Burnup and Temperature

$$F = \exp [Y_o + K_1 T + K_2 T^2 + K_3 T^3 + K_4 T^4 + K_5 B + K_6 BT + K_7 BT^2 + K_8 BT^3 + K_9 BT^4 + K_{10} B^2 + K_{11} B^2 T + K_{12} B^2 T^2 + K_{13} B^2 T^3 + K_{14} B^2 T^4 + K_{15} B^3 + K_{16} B^3 T + K_{17} B^3 T^2 + K_{18} B^3 T^3 + K_{19} B^3 T^5 + K_{20} B^4 + K_{21} B^4 T + K_{22} B^4 T^2 + K_{23} B^4 T^4 + K_{24} B^5 + K_{25} B^5 T + K_{26} B^5 T^2 + K_{27} B^5 T^5]$$

F = % fission gas release

B = burnup in atom %

T = temperature in °K

$R^2 = 0.999975$

Grainsize = 10 microns

Temperature gradient = -2000°C/cm

$Y_o = 41.80378709$

$K_1 = -0.0688818$	$K_{10} = -36.80973733$	$K_{19} = 7.4414626 \times 10^{-17}$
$K_2 = 2.2256317 \times 10^{-5}$	$K_{11} = 0.09886291$	$K_{20} = -0.494793$
$K_3 = 7.7409021 \times 10^{-9}$	$K_{12} = -0.00010015$	$K_{21} = 0.00066996$
$K_4 = -3.3257020 \times 10^{-12}$	$K_{13} = 4.2968059 \times 10^{-8}$	$K_{22} = -2.9976856 \times 10^{-7}$
$K_5 = 82.06280479$	$K_{14} = -6.5986406 \times 10^{-12}$	$K_{23} = 1.7773771 \times 10^{-14}$
$K_6 = -0.2430218$	$K_{15} = 4.89700225$	$K_{24} = 0.03681195$
$K_7 = 0.00026376$	$K_{16} = -0.01020471$	$K_{25} = -4.7977 \times 10^{-5}$
$K_8 = -1.1926854 \times 10^{-7}$	$K_{17} = 8.3021159 \times 10^{-6}$	$K_{26} = 1.8615955 \times 10^{-8}$
$K_9 = 1.9118314 \times 10^{-11}$	$K_{18} = -2.4521160 \times 10^{-9}$	$K_{27} = -3.4968851 \times 10^{-19}$

TABLE X. Correlation for Gas Release as a Function of Burnup and Temperature Gradient

$$F = \exp [Y_o + K_1 G + K_2 G^2 + K_3 B + K_4 BG + K_5 BG^2 + K_6 B^2 + K_7 B^2 G + K_8 B^2 G^2 + K_9 B^3 + K_{10} B^3 G + K_{11} B^3 G^2 + K_{12} B^4 + K_{13} B^4 G + K_{14} B^4 G^2 + K_{15} B^5 + K_{16} B^5 G + K_{17} B^5 G^2]$$

F = % fission gas release

B = burnup in atom %

G = temperature gradient in °C/cm

$R^2 = 0.999815$

Temperature = 2000°K

Grain Size = 10 microns

$Y_o = 1.64402267$

$K_1 = -0.00020062$

$K_2 = -6.3923114 \times 10^{-8}$

$K_3 = 3.4424575$

$K_4 = 0.00065915$

$K_5 = 1.685822 \times 10^{-7}$

$K_6 = -2.09779214$

$K_7 = -0.00056867$

$K_8 = -1.4542974 \times 10^{-7}$

$K_9 = 0.67725119$

$K_{10} = 0.00021815$

$K_{11} = 5.6828958 \times 10^{-8}$

$K_{12} = -0.10887743$

$K_{13} = -3.9051822 \times 10^{-5}$

$K_{14} = -1.0339969 \times 10^{-8}$

$K_{15} = 0.00683431$

$K_{16} = 2.6450757 \times 10^{-6}$

$K_{17} = 7.0858151 \times 10^{-10}$

TABLE XI. Correlation for Gas Release as a Function of Temperature and Grain Size

$$F = \exp [Y_o + K_1 S + K_2 S^2 + K_3 S^3 + K_4 T + K_5 TS + K_6 TS^2 + K_7 TS^3 + K_8 T^2 + K_9 T^2 S + K_{10} T^2 S^2 + K_{11} T^2 S^3 + K_{12} T^3 + K_{13} T^3 S + K_{14} T^3 S^2 + K_{15} T^3 S^3 + K_{16} T^4 + K_{17} T^4 S + K_{18} T^4 S^2]$$

F = % fission gas release

T = temperature in °K

S = grainsize in microns

$R^2 = 1.000000$

Burnup = 3.0

Temperature Gradient = -2000°C/cm

$Y_o = -258.50642181$

$K_1 = 54.43264259$

$K_2 = -2.41609916$

$K_3 = 0.03245449$

$K_4 = 0.64832039$

$K_5 = -0.13846319$

$K_6 = 0.00613152$

$K_7 = -7.9214382 \times 10^{-5}$

$K_8 = -0.00058169$

$K_9 = 0.00012659$

$K_{10} = -5.5588263 \times 10^{-6}$

$K_{11} = 6.6410060 \times 10^{-8}$

$K_{12} = 2.2420110 \times 10^{-7}$

$K_{13} = -4.9186863 \times 10^{-8}$

$K_{14} = 2.0939154 \times 10^{-9}$

$K_{15} = -2.0218726 \times 10^{-11}$

$K_{16} = -3.069132 \times 10^{-11}$

$K_{17} = 6.6124027 \times 10^{-12}$

$K_{18} = -2.4305576 \times 10^{-13}$

TABLE XII. Correlation for Gas Release as a Function of Temperature and Temperature Gradient

$$F = \exp[Y_o + K_1G + K_2G^2 + K_3T + K_4TG + K_5TG^2 + K_6T^2 + K_7T^2G + K_8T^2G^2 + K_9T^3 + K_{10}T^3G + K_{11}T^3G^2 + K_{12}T^4 + K_{13}T^4G]$$

F = % fission gas release

T = temperature in °K

G = temperature gradient in °C/cm

$R^2 = 1.000000$

Burnup = 3.0 atom %

Grain Size = 10 microns

$Y_o = 147.62346999$	$K_5 = -1.216478 \times 10^{-9}$	$K_{10} = -3.1089465 \times 10^{-11}$
$K_1 = 0.03606444$	$K_6 = 0.00035681$	$K_{11} = -1.5819461 \times 10^{-16}$
$K_2 = 6.1519885 \times 10^{-7}$	$K_7 = 8.0097042 \times 10^{-8}$	$K_{12} = 2.0855405 \times 10^{-11}$
$K_3 = -0.37985633$	$K_8 = 7.713925 \times 10^{-13}$	$K_{13} = 4.4116346 \times 10^{-15}$
$K_4 = -8.9146867 \times 10^{-5}$	$K_9 = -1.4307505 \times 10^{-7}$	

TABLE XIII. Correlation for Gas Release as a Function of Grain Size and Temperature Gradient

$$F = \exp[Y_o + K_1G + K_2G^2 + K_3S + K_4SG + K_5SG^2 + K_6S^2 + K_7S^2G + K_8S^2G^2 + K_9S^3 + K_{10}S^3G + K_{11}S^3G^2]$$

F = % fission gas release

S = Grain size in microns

G = temperature gradient in °C/cm

$R^2 = 1.000000$

Burnup = 3.0 atom %

Temperature = 2000°K

$Y_o = 4.0539659$

$K_1 = 9.5914047 \times 10^{-5}$	$K_5 = 7.8469977 \times 10^{-9}$	$K_9 = -2.8255144 \times 10^{-5}$
$K_2 = -3.6105216 \times 10^{-8}$	$K_6 = 0.00110985$	$K_{10} = -6.1459985 \times 10^{-9}$
$K_3 = 0.00859075$	$K_7 = 6.1488661 \times 10^{-7}$	$K_{11} = 1.0565916 \times 10^{-11}$
$K_4 = -1.2194361 \times 10^{-5}$	$K_8 = -5.0674558 \times 10^{-10}$	

TABLE XIV. Number of Variables To Be Considered

Number of Parameters	Number of Variables
1	5
2	35
3	215
4	1295

One method was tried that is relatively easy to use and gives good results. Consider the development of a three-parameter correlation with independent variables of temperature, burnup, and grain size. It is relatively easy to construct the correlations for combinations of two variables. For the three variables being considered, the correlations are described in Tables VII and X. All the variables in the correlations for two parameters should be included in the three-parameter correlation, since it has been shown they are significant in at least one equation. Then the relationships between the variables should be analyzed to identify significant three-variable combinations. There is a relatively easy straightforward method for doing this. First, construct a chart of two variables, as illustrated in Table XV for temperature and burnup. Then, use Table IX to identify and mark out those squares that are not related, as shown in Table XVI. By cross-referencing burnup and temperature in the chart with Tables VII and XII, fill in the chart with grain sizes that match, as shown in Table XVII. Table XVIII is the expanded form of Table XVII and contains all the three-variable combinations that should be considered in the model for a three-parameter correlation.

The parametric model for three variables as described above is shown as Table XIX. The method was tested by developing a model considering all possible variables. The results are shown in Table XX. The results between the two methods are comparable.

TABLE XV. Two-variable Chart for Three Significant Parameter Variable Development Method

	T	T^2	T^3	T^4	T^5
B					
B^2					
B^3					
B^4					
B^5					

TABLE XVI. Correlating Variables in Two-variable Chart

	T	T^2	T^3	T^4	T^5
B					---
B^2					---
B^3				---	
B^4			---		---
B^5			---	---	

TABLE XVII. Completed Two-variable Chart

	T	T^2	T^3	T^4	T^5
B	SS^2S^3	SS^2S^3	SS^2S^3	SS^2	---
B^2	SS^2S^3	SS^2S^3	SS^2S^3	SS^2	---
B^3	SS^2S^3	SS^2S^3	SS^2S^3	---	
B^4	SS^2S^3	SS^2S^3	---	SS^2	---
B^5	SS^2	SS^2	---	---	

TABLE XVIII. Significant Three-parameter Variables

BTS	BT^2S	BT^3S	BT^4S	---
BTS^2	BT^2S^2	BT^3S^2	BT^4S^2	---
BTS^3	BT^2S^3	BT^3S^3	---	---
B^2TS	B^2T^2S	B^2T^3S	B^2T^4S	---
B^2TS^2	$B^2T^2S^2$	$B^2T^3S^2$	$B^2T^4S^2$	---
B^2TS^3	$B^2T^2S^3$	$B^2T^3S^3$	---	---
B^3TS	B^3T^2S	B^3T^3S	---	---
B^3TS^2	$B^3T^2S^2$	$B^3T^3S^2$	---	---
B^3TS^3	$B^3T^2S^3$	$B^3T^3S^3$	---	---
B^4TS	B^4T^2S	---	B^4T^4S	---
B^4TS^2	$B^4T^2S^2$	---	$B^4T^4S^2$	---
B^4TS^3	$B^4T^2S^3$	---	---	---
B^5TS	B^5T^2S	---	---	---
B^5TS^2	$B^5T^2S^2$	---	---	---
---	---	---	---	---

TABLE XIX. Correlation for Fission-gas Release as Function of Burnup, Temperature, and Grain Size Using Two-variable-chart Method

$$
\begin{aligned}
F = \exp [Y_o &+ K_1 S + K_2 S^2 + K_3 S^3 + K_4 TS + K_5 TS^2 \\
&+ K_6 TS^3 + K_7 T + K_8 T^2 S + K_9 T^2 S^2 + K_{10} T^2 S^3 \\
&+ K_{11} T^2 + K_{12} T^3 S + K_{13} T^3 S^2 + K_{14} T^3 S^3 + K_{15} T^3 \\
&+ K_{16} T^4 S + K_{17} T^4 S^2 + K_{18} T^4 + K_{19} BS + K_{20} BS^2 \\
&+ K_{21} BS^3 + K_{22} B + K_{23} BTS + K_{24} BTS^2 + K_{25} BTS^3 \\
&+ K_{26} BT + K_{27} BT^2 S + K_{28} BT^2 S^2 + K_{29} BT^2 S^3 + K_{30} BT^2 \\
&+ K_{31} BT^3 S + K_{32} BT^3 S^2 + K_{33} BT^3 S^3 + K_{34} BT^3 + K_{35} BT^4 S \\
&+ K_{36} BT^4 + K_{37} B^2 S + K_{38} B^2 S^2 + K_{39} B^2 S^3 + K_{40} B^2 \\
&+ K_{41} B^2 TS + K_{42} B^2 TS^2 + K_{43} B^2 TS^3 + K_{44} B^2 T + K_{45} B^2 T^2 S \\
&+ K_{46} B^2 T^2 S^2 + K_{47} B^2 T^2 S^3 + K_{48} B^2 T^2 + K_{49} B^2 T^3 S + K_{50} B^2 T^3 S^2 \\
&+ K_{51} B^2 T^3 + K_{52} B^2 T^4 S + K_{53} B^3 S + K_{54} B^3 S^2 + K_{55} B^3 S^3 \\
&+ K_{56} B^3 + K_{57} B^3 TS + K_{58} B^3 TS^2 + K_{59} B^3 TS^3 + K_{60} B^3 T \\
&+ K_{61} B^3 T^2 S + K_{62} B^3 T^2 S^2 + K_{63} B^3 T^2 S^3 + K_{64} B^3 T^2 + K_{65} B^3 T^3 S \\
&+ K_{66} B^3 T^3 + K_{67} B^3 T^5 + K_{68} B^4 S + K_{69} B^4 S^2 + K_{70} B^4 S^3 \\
&+ K_{71} B^4 + K_{72} B^4 TS + K_{73} B^4 TS^2 + K_{74} B^4 TS^3 + K_{75} B^4 T \\
&+ K_{76} B^4 T^2 S + K_{77} B^4 T^2 S^2 + K_{78} B^4 T^2 + K_{79} B^4 T^4 S + K_{80} B^4 T^4 S^2 \\
&+ K_{81} B^4 T^4 + K_{82} B^5 S + K_{83} B^5 S^2 + K_{84} B^5 S^4 + K_{85} B^5 \\
&+ K_{86} B^5 TS + K_{87} B^5 TS^2 + K_{88} B^5 T + K_{89} B^5 T^2 S + K_{90} B^5 T^5
\end{aligned}
$$

F = % fission gas release

B = Burnup in atom .%

T = Average temperature in °K

S = Grain size in microns

$R^2 = 0.999562$

Temperature Gradient = -2000°C/cm

TABLE XIX (Contd.)

Y_o = 165.97038883

K_1 = 0.35235412
K_2 = -0.69067757
K_3 = 0.0052581
K_4 = 0.00349255
K_5 = 0.0015288
K_6 = $-9.7364022 \times 10^{-6}$
K_7 = -0.40286859
K_8 = $-7.2742205 \times 10^{-6}$
K_9 = $-1.2117416 \times 10^{-6}$
K_{10} = 5.6897573×10^{-9}
K_{11} = 0.00034878
K_{12} = 4.3286311×10^{-9}
K_{13} = $4.1217353 \times 10^{-10}$
K_{14} = $-1.0558463 \times 10^{-12}$
K_{15} = $-1.2869615 \times 10^{-7}$
K_{16} = $-8.0179822 \times 10^{-13}$
K_{17} = $-5.1333047 \times 10^{-14}$
K_{18} = $1.7249638 \times 10^{-11}$
K_{19} = 18.57178331
K_{20} = 0.11968614
K_{21} = -0.00280718
K_{22} = -219.12189647
K_{23} = -0.04816678
K_{24} = -0.00013588
K_{25} = 4.0160902×10^{-6}
K_{26} = 0.50052969
K_{27} = 4.3682559×10^{-5}
K_{28} = 4.4311549×10^{-8}
K_{29} = $-1.8735592 \times 10^{-9}$
K_{30} = -0.0003918
K_{31} = $-1.6686918 \times 10^{-8}$
K_{32} = $-3.0163208 \times 10^{-12}$
K_{33} = $2.7584091 \times 10^{-13}$
K_{34} = 1.2709933×10^{-7}
K_{35} = $2.2902315 \times 10^{-12}$
K_{36} = -1.43986×10^{-11}
K_{37} = -4.71860548
K_{38} = -0.01060209
K_{39} = 0.00046776
K_{40} = 57.16161684
K_{41} = 0.01169398
K_{42} = $-1.5457865 \times 10^{-5}$
K_{43} = -3.706507×10^{-7}
K_{44} = -0.11910016
K_{45} = $-9.6268797 \times 10^{-6}$
K_{46} = 1.8261541×10^{-8}
K_{47} = 8.807547×10^{-11}
K_{48} = 7.4900831×10^{-5}
K_{49} = 3.2098382×10^{-9}
K_{50} = $-4.4040632 \times 10^{-12}$
K_{51} = $-1.4884413 \times 10^{-8}$
K_{52} = $-3.6674644 \times 10^{-13}$
K_{53} = 0.30239382
K_{54} = 0.00410962
K_{55} = $-6.6271669 \times 10^{-5}$
K_{56} = -7.76486359
K_{57} = -0.00083933
K_{58} = $-7.1069891 \times 10^{-7}$
K_{59} = 2.5109161×10^{-8}
K_{60} = 0.01700807
K_{61} = 6.0150535×10^{-7}
K_{62} = $-2.4210479 \times 10^{-10}$
K_{63} = $-3.6025413 \times 10^{-12}$
K_{64} = $-9.9404539 \times 10^{-6}$
K_{65} = $-1.2925061 \times 10^{-10}$
K_{66} = 1.4716429×10^{-9}
K_{67} = $5.9922553 \times 10^{-17}$
K_{68} = 0.01741106
K_{69} = -0.00069754
K_{70} = 6.2681947×10^{-6}
K_{71} = 0.29868161
K_{72} = 1.1640639×10^{-6}
K_{73} = 4.2672833×10^{-7}
K_{74} = $-8.3138055 \times 10^{-10}$
K_{75} = -0.00102524
K_{76} = $-9.0963609 \times 10^{-9}$
K_{77} = $-1.5471419 \times 10^{-10}$
K_{78} = 6.0793105×10^{-7}
K_{79} = $1.1393432 \times 10^{-15}$
K_{80} = $1.1436358 \times 10^{-17}$
K_{81} = $-4.4473431 \times 10^{-14}$
K_{82} = -0.00292805
K_{83} = 1.9981552×10^{-5}
K_{84} = $-3.7995119 \times 10^{-9}$
K_{85} = 0.02989121
K_{86} = 3.1891436×10^{-6}
K_{87} = $-4.9456473 \times 10^{-9}$
K_{88} = $-1.8518522 \times 10^{-5}$
K_{89} = $-8.7813928 \times 10^{-10}$
K_{90} = $2.8398323 \times 10^{-19}$

TABLE XX. Correlation for Fission-gas Release as Function of Burnup, Temperature, and Grain Size Considering All Possible Variables

$$
\begin{aligned}
F = \exp [Y_o &+ K_1 S + K_2 S^2 + K_3 S^3 + K_4 TS + K_5 TS^2 \\
&+ K_6 TS^3 + K_7 TS^4 + K_8 T^2 S + K_9 T^2 S^2 + K_{10} T^2 S^3 \\
&+ K_{11} T^2 S^4 + K_{12} T^3 S + K_{13} T^3 S^2 + K_{14} T^3 S^3 + K_{15} T^3 S^5 \\
&+ K_{16} T^4 S + K_{17} T^4 S^2 + K_{18} T^4 S^5 + K_{19} T^4 + K_{20} BS \\
&+ K_{21} BS^2 + K_{22} BS^3 + K_{23} BS^4 + K_{24} BTS + K_{25} BTS^2 \\
&+ K_{26} BTS^3 + K_{27} BTS^4 + K_{28} BT^2 S + K_{29} BT^2 S^2 + K_{30} BT^2 S^3 \\
&+ K_{31} BT^2 S^4 + K_{32} BT^3 S + K_{33} BT^3 S^2 + K_{34} BT^3 S^3 + K_{35} BT^3 \\
&+ K_{36} BT^4 S + K_{37} BT^4 S^3 + K_{38} BT^4 + K_{39} B^2 S + K_{40} B^2 S^2 \\
&+ K_{41} B^2 S^3 + K_{42} B^2 S^4 + K_{43} B^2 TS + K_{44} B^2 TS^2 + K_{45} B^2 TS^3 \\
&+ K_{46} B^2 TS^4 + K_{47} B^2 T^2 S + K_{48} B^2 T^2 S^2 + K_{49} B^2 T^2 S^3 + K_{50} B^2 T^2 S^5 \\
&+ K_{51} B^2 T^3 S + K_{52} B^2 T^3 S^2 + K_{53} B^2 T^3 S^4 + K_{54} B^2 T^3 + K_{55} B^2 T^4 S \\
&+ K_{56} B^2 T^5 S^2 + K_{57} B^2 T^5 S^4 + K_{58} B^2 T^5 + K_{59} B^3 S + K_{60} B^3 S^2 \\
&+ K_{61} B^3 S^3 + K_{62} B^3 S^4 + K_{63} B^3 TS + K_{64} B^3 TS^2 + K_{65} B^3 TS^3 \\
&+ K_{66} B^3 TS^5 + K_{67} B^3 T^2 S + K_{68} B^3 T^2 S^2 + K_{69} B^3 T^2 S^3 + K_{70} B^3 T^2 \\
&+ K_{71} B^3 T^3 S + K_{72} B^3 T^3 S^3 + K_{73} B^3 T^3 + K_{74} B^3 T^5 S + K_{75} B^4 S \\
&+ K_{76} B^4 S^2 + K_{77} B^4 S^3 + K_{78} B^4 S^5 + K_{79} B^4 TS + K_{80} B^4 TS^2 \\
&+ K_{81} B^4 TS^3 + K_{82} B^4 T + K_{83} B^4 T^2 S + K_{84} B^4 T^2 S^2 + K_{85} B^4 T^2 \\
&+ K_{86} B^4 T^3 S^5 + K_{87} B^4 T^4 S + K_{88} B^4 T^4 + K_{89} B^4 T^5 S^3 + K_{90} B^4 T^5 S^5 \\
&+ K_{91} B^5 S + K_{92} B^5 S^2 + K_{93} B^5 S^3 + K_{94} B^5 + K_{95} B^5 TS \\
&+ K_{96} B^5 TS^2 + K_{97} B^5 T + K_{98} B^5 T^2 S + K_{99} B^5 T^2 S^5 + K_{100} B^5 T^3 \\
&+ K_{101} B^5 T^4 S^3]
\end{aligned}
$$

F = % fission gas release T = Average temperature in °K R^2 = 0.999896

B = Burnup in atom % S = Grain size in microns Temperature gradient = -2000°C/cm

TABLE XX (Contd.)

$Y_o = 148.18763811$

$K_1 = 11.0713666$

$K_2 = -2.28102435$

$K_3 = 0.04468$

$K_4 = -0.16300176$

$K_5 = 0.02261453$

$K_6 = -0.0009035$

$K_7 = 1.2241621 \times 10^{-5}$

$K_8 = 0.00013904$

$K_9 = -1.9828387 \times 10^{-5}$

$K_{10} = 7.9217951 \times 10^{-7}$

$K_{11} = -1.0723809 \times 10^{-8}$

$K_{12} = -4.862309 \times 10^{-8}$

$K_{13} = 6.7097779 \times 10^{-9}$

$K_{14} = -2.094089 \times 10^{-10}$

$K_{15} = 6.1212201 \times 10^{-14}$

$K_{16} = -7.9860390 \times 10^{-13}$

$K_{17} = -1.151604 \times 10^{-13}$

$K_{18} = 1.8207537 \times 10^{-18}$

$K_{19} = 1.9572401 \times 10^{-11}$

$K_{20} = -85.38880205$

$K_{21} = 14.99721006$

$K_{22} = -0.70309480$

$K_{23} = 0.01056369$

$K_{24} = 0.20007261$

$K_{25} = -0.03619622$

$K_{26} = 0.00170588$

$K_{27} = -2.57023 \times 10^{-5}$

$K_{28} = -0.00016224$

$K_{29} = 3.0592787 \times 10^{-5}$

$K_{30} = -1.4463146 \times 10^{-6}$

$K_{31} = 2.1806881 \times 10^{-8}$

$K_{32} = -3.4712421 \times 10^{-8}$

$K_{33} = -5.1315365 \times 10^{-12}$

$K_{34} = 1.052556 \times 10^{-11}$

$K_{35} = 2.3466344 \times 10^{-7}$

$K_{36} = 4.9194665 \times 10^{-12}$

$K_{37} = -1.4199714 \times 10^{-15}$

$K_{38} = -3.0320612 \times 10^{-11}$

$K_{39} = 17.90475827$

$K_{40} = -3.47545479$

$K_{41} = 0.16214193$

$K_{42} = -0.00241314$

$K_{43} = -0.03938004$

$K_{44} = 0.00821365$

$K_{45} = -0.00038741$

$K_{46} = 5.8115135 \times 10^{-6}$

$K_{47} = 2.2449317 \times 10^{-5}$

$K_{48} = -5.3055343 \times 10^{-6}$

$K_{49} = 1.9439466 \times 10^{-7}$

$K_{50} = -6.6364556 \times 10^{-11}$

$K_{51} = 9.8432227 \times 10^{-9}$

$K_{52} = -3.0741301 \times 10^{-11}$

$K_{53} = -2.946215 \times 10^{-14}$

$K_{54} = -3.3482192 \times 10^{-8}$

$K_{55} = -1.3062439 \times 10^{-12}$

$K_{56} = 5.1693338 \times 10^{-19}$

$K_{57} = 8.1287935 \times 10^{-22}$

$K_{58} = 6.3848254 \times 10^{-16}$

$K_{59} = -1.40732201$

$K_{60} = 0.22532707$

$K_{61} = -0.00984288$

$K_{62} = 0.00013859$

$K_{63} = 0.00438461$

$K_{64} = -0.00069009$

$K_{65} = 2.4950002 \times 10^{-5}$

$K_{66} = -8.4659375 \times 10^{-9}$

$K_{67} = 1.6980446 \times 10^{-6}$

$K_{68} = 3.5136428 \times 10^{-10}$

$K_{69} = -5.6391945 \times 10^{-10}$

$K_{70} = -1.3344323 \times 10^{-5}$

$K_{71} = -4.8634033 \times 10^{-10}$

$K_{72} = 1.2885372 \times 10^{-13}$

$K_{73} = 3.0466537 \times 10^{-9}$

$K_{74} = 1.0961448 \times 10^{-17}$

$K_{75} = -0.17253031$

$K_{76} = 0.03137199$

$K_{77} = -0.00123745$

TABLE XX (Contd.)

$K_{78} = 4.6627034 \times 10^{-7}$	$K_{86} = 1.0464379 \times 10^{-18}$	$K_{94} = 0.0988793$
$K_{79} = -0.00012118$	$K_{87} = 1.5707688 \times 10^{-15}$	$K_{95} = 1.2078907 \times 10^{-5}$
$K_{80} = 3.1816258 \times 10^{-6}$	$K_{88} = -3.971347 \times 10^{-14}$	$K_{96} = -1.4427662 \times 10^{-7}$
$K_{81} = -4.1694528 \times 10^{-8}$	$K_{89} = -3.3099291 \times 10^{-22}$	$K_{97} = -7.6762587 \times 10^{-5}$
$K_{82} = 0.00030467$	$K_{90} = -1.3730585 \times 10^{-25}$	$K_{98} = -2.7154551 \times 10^{-9}$
$K_{83} = 1.0506929 \times 10^{-8}$	$K_{91} = -0.01321431$	$K_{99} = 2.2541389 \times 10^{-16}$
$K_{84} = -1.2891514 \times 10^{-11}$	$K_{92} = 0.00033438$	$K_{100} = 6.74426 \times 10^{-12}$
$K_{85} = 2.4362412 \times 10^{-7}$	$K_{93} = -3.2959239 \times 10^{-6}$	$K_{101} = 6.7807178 \times 10^{-20}$

d. Conclusions

Parametric correlations of two and three variables have been developed to describe GRASS-SST-predicted steady-state fission-gas release from UO_2-based fuels. The parametric model, PARAGRASS, has the capability of reproducing GRASS-SST results with good accuracy. In future work, other parameters will be included in the model, and the model will be extended to transient analyses. Also, the methods used to develop correlations for fission-gas release will be used to develop correlations for fuel-swelling strain. An assumption used in the GRASS-SST calculation of grain-edge swelling has been found deficient and is being replaced with a more realistic model.

C. Experimental Program (S. M. Gehl, MSD)

1. Posttest Characterization of ORNL Specimens

At the request of the NRC, irradiated fuel specimens tested in the program "Fission Product Behavior in LWRs" at ORNL are being examined at ANL-East. The examination is intended to provide an explanation for the high release fractions of volatile fission products in tests at temperatures greater than 1300°C. Before describing the preliminary findings of the posttest characterization, we will summarize relevant aspects of the ORNL program and results.

The release of fission products from irradiated LWR fuel during LOCA conditions was studied at ORNL by heating segments of fuel in a steam-containing atmosphere. Fission products escaped from the rods through drilled holes or ruptures caused by internal pressurization of the cladding. Quantitative determinations were made of the release of several fission-product isotopes.[3-5]

The experimental results showed that high release fractions of cesium and iodine occurred for test temperatures greater than 1350°C.[3,4] The high release values could not be explained by diffusion along the fuel-cladding gap or through the UO_2 matrix.[5] Release via interconnected grain-boundary tunnels was proposed as an explanation for the observed release fractions.[7] This proposal was made by analogy with the presence of interconnected tunnels in other systems.[6-8]

To check on the validity of the tunnel interconnection hypothesis, as well as to determine whether other gas-release mechanisms were also operative, selected specimens from the ORNL program were sent to ANL-East for characterization of the posttest microstructures and fission-product distribution. The specimens were taken from the same H. B. Robinson bundle used as the source for the fuel tested in the ANL-DEH program. The test conditions represented by the ORNL specimens sent to ANL-East are listed in Table XXI, which also contains the measured values of fission-product release for the tests.

TABLE XXI. Test Conditions and Fission-product Release for Specimens Sent to ANL-East[5-7]

Test No.	Method of Cladding Breaching	Heating Method	Heatup Rate, °C/s	Cladding Surface Temperature, °C	Test Period, min	Percent of Total Inventory Released[a]		
						^{85}Kr	^{134}Cs	^{129}I
HBU-10	Rupture	Induction	3	1200	10	3.4	0.12	0.066
HBU-11[b]	Rupture	Resistance heater	0.7	1200	10	2.6[c]	0.024	0.036
HT-1	Drilled hole	Induction	9	~1300	10	2.1 + 0.5[d]	0.22	0.33
HT-2	Drilled hole	Induction	8	~1445	7	10.0 + 1.0[d]	9.64	4.70
HT-3	Drilled hole	Induction	9	~1610	3	16.6 + 1.0[a]	16.5	-
HT-4	Drilled hole	Induction	14	~1400	0.33	5.6 + 1.5[d]	6.2	3.6

[a]Based on a heated length of 15.2-16.5 cm.
[b]Total test time was 27 min; release values were adjusted for a 10-min period.
[c]Includes ^{85}Kr released when this segment was used in a previous test at 900°C, Test HBU-7.
[d]Estimated release during cladding expansion.

The data show a large increase in fission-product release between 1300 and 1400°C. (Since the temperature reached 1350°C for ~2 min during Test HT-1, the jump in fission-product release is probably in the range of 1350-1400°C.) Note that specimens tested at above and below the transition range are available for comparison. The former tests are labeled HT- for "high temperature"; the latter are labeled HBU- for "high burnup." Note, however, that the burnups are the same for the HT and HBU series.

The objective of the ANL-East examination is to determine the mechanisms of fission-gas release in the high-temperature test sepcimens. The examination was planned to consist of microstructural studies of bubbles, microcracks, and other features related to the redistribution and release of fission products; and direct measurements of the posttest radial profiles of fission gases and volatile fission products. The results of this characterization are to be compared with previously obtained information on untested and DEH-tested fuels.

This study is particularly important because the heating of ruptured fuel rods in a steam atmosphere is similar in certain respects to the TMI-2 accident. The potential application of the present study to the understanding of the TMI-2 accident sequence will influence the course of the posttest examination and the evaluation of the results.

a. Condition of Specimens Received at ANL-East

When the ORNL tests were completed, the specimens were stored in heavy-walled storage tubes. Specimens HBU-10 and -11 were kept in an indoor storage vault; specimens HT-1, -2, -3, and -4 were placed in a second container and moved to a burial site. When these specimens were retrieved from the burial ground, a small amount of water was found inside the outer container. Chemical analysis of the water did not reveal the presence of fission products, suggesting that the water did not come in contact with the fuel.[9] However, water vapor may have contacted the fuel specimens through openings in the storage tubes and affected the chemical state or distribution of some fission products.

The specimens themselves were not inspected before shipment. When the storage tubes were opened at ANL-East, the Zircaloy claddings of all the specimens were found to be fractured into several large, and many smaller, pieces. The oxidized cladding was extremely brittle and may have fractured at any time during handling or shipment. Without intact cladding to retain their relative positions, the fuel-pellet chunks were free to tumble about within the storage tubes. Therefore, all information as to the axial location of the fuel chunks, e.g., relative to the cladding breach, was lost.

The appearance of the HT-2 specimen after removal from the storage tube is shown in Figs. 8 and 9. A small amount of fuel remained within the cladding pieces near the end fittings. However, this fuel was outside the

heated zone of the specimen and experienced relatively little temperature increase during the experiment. All the fuel chunks from the hot zone as well as many of the smaller cladding fragments are visible in Fig. 9. The size and morphology of the fuel chunks are the same as was observed in the postirradiation examination of the H. B. Robinson fuel. Little, if any, breakage occurred as a result of handling and shipping.

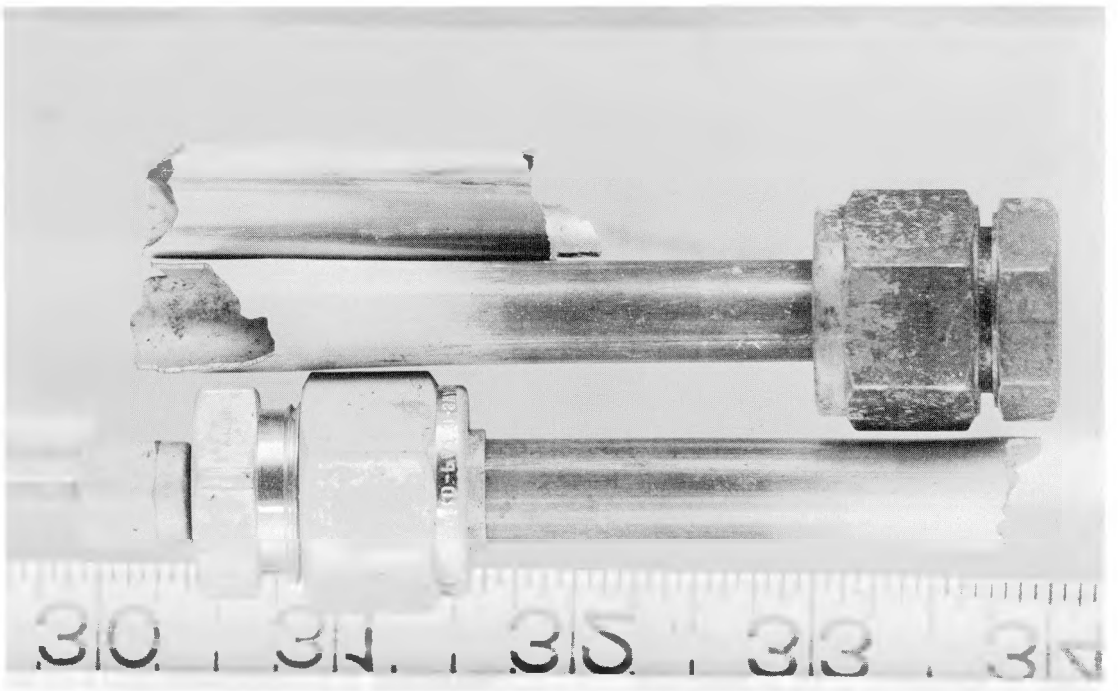

Fig. 8. Large Cladding Pieces and End Fittings of the HT-2 Test Specimen. Neg. No. MSD-222020.

Fig. 9. Small Fuel and Cladding Pieces of the HT-2 Test Specimen. Neg. Nos. MSD-222018 and -222019.

The loose mixture of fuel chunks and cladding fragments was found in all the storage tubes. The only readily apparent difference among the specimens is that fewer small cladding pieces were observed for the low-temperature specimens.

b. Preliminary Examination Results

The as-received condition of the test specimen makes the systematic characterization of the fuel and cladding difficult. Constraints of time and funding dictate that only a limited number of samples from each specimen can be examined.

For the fuel microstructures, the sampling problem was addressed by selecting two of the larger chunks from each test specimen. Each chunk was oriented in a metallographic mount so that the axis of the original fuel pellet was perpendicular to the plane of polish. After being ground to expose a transverse cross section, the chunks were polished and examined in the optical microscope. Several of the resulting sections are reproduced in Figs. 10-12.

Several of the sections exhibited intergranular microcracking similar to that observed during both nuclear and direct-electrical heating of irradiated oxide fuels.[6,7] For Test HBU-10, microcracks were oriented circumferentially and were limited to a zone ~0.16 mm in from the outer-pellet radius. Microcracking was not observedin the two sections examined from Test HT-1. General microcracking, i.e., not limited to the fuel periphery, was observed in Tests HT-2 and -3. However, as shown in Fig. 12, the density of microcracks

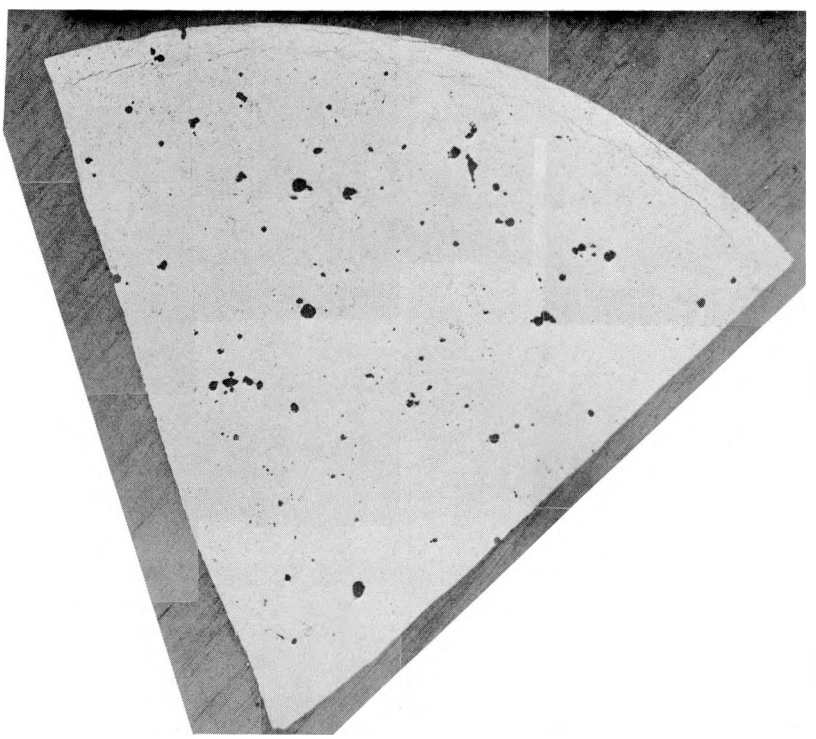

Fig. 10. Transverse Section through a Fuel Chunk of the HBU-10 Test Specimen. Neg. No. MSD-222148

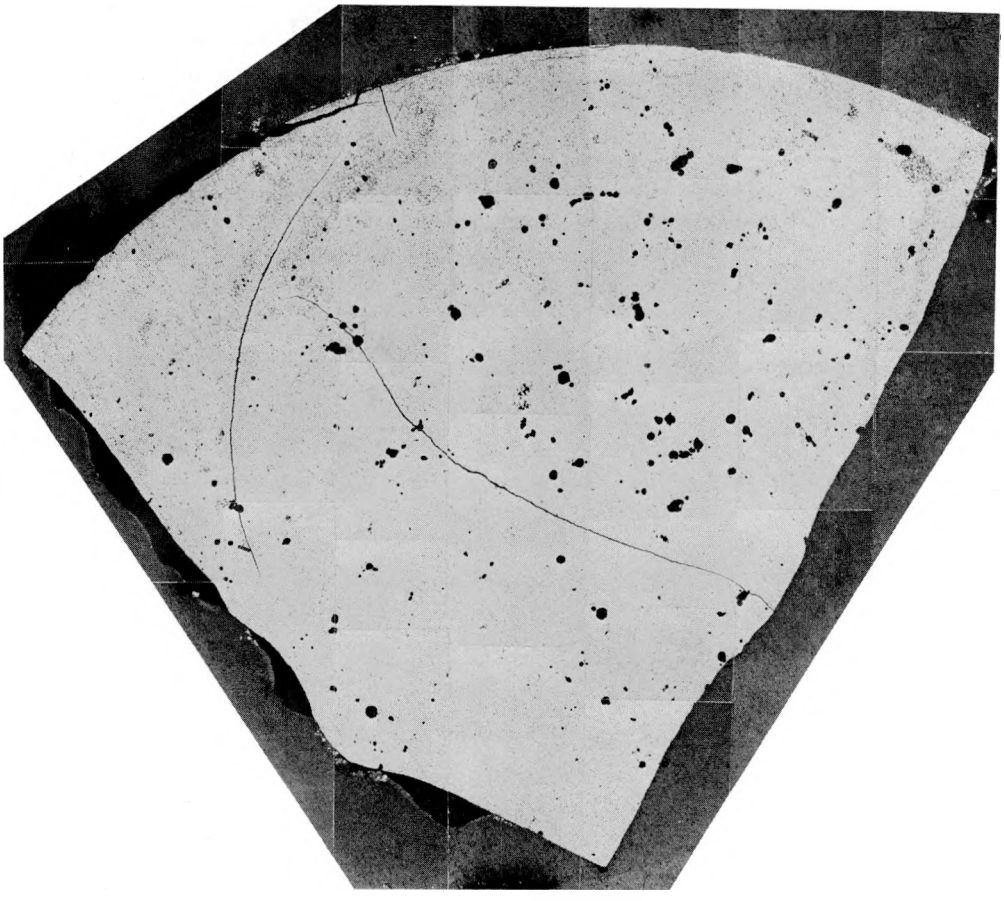

Fig. 11. Transverse Section through a Fuel Chunk of the HT-1 Test Specimens. ANL Neg. No. 222147.

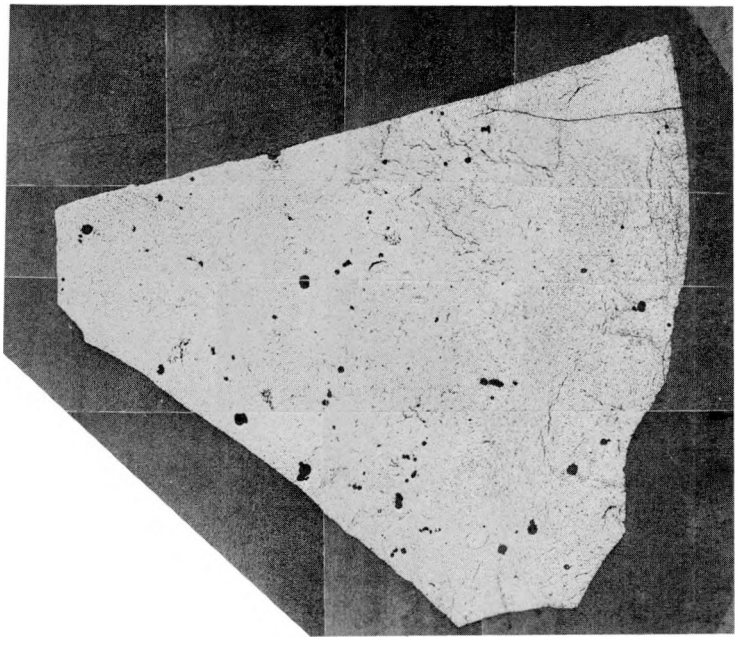

Fig. 12. Transverse Section through a Fuel Chunk of the HT-2 Test Specimens. Neg. No. MSD-222152.

was highest near the pellet periphery and decreased toward the center. Because of the problems in sampling, the absence of microcracks on the sections examined does not indicate that microcracking did not occur in a particular test. Similarly the presence of a limited amount of microcracking (see Fig. 10) does not indicate that microcracking was an important mechanism of fission-product release. The only conclusion that can be drawn from the present results is that microcracking has occurred in several of the tests and that it has presumably contributed to fission-product release.

In the HT-2 and -3 specimens, fuel particles were sometimes attached to the cladding. The most notable example of this phenomenon, taken from the Test HT-2 is shown in Fig. 13. This specimen consists of an ~47-mm-long piece of cladding, which fractured lengthwise to expose several chunks of fuel attached to the inner cladding surface.

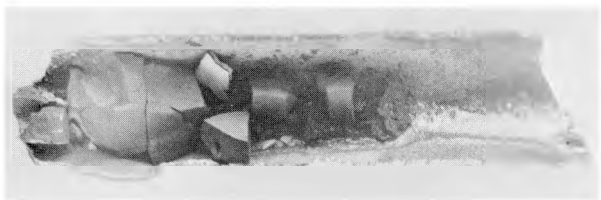

Fig. 13. Fuel Chunks Attached to a Cladding Segment HT-2 Test Specimen. Neg. No. MSD-222022.

A transverse section through the fuel-containing region is shown in Fig. 14. A thick layer of oxide formed at the outer surface of the cladding. The oxide layer varies between 0.22 and 0.6 mm in thickness, compared with the original cladding thickness of 0.617 mm.

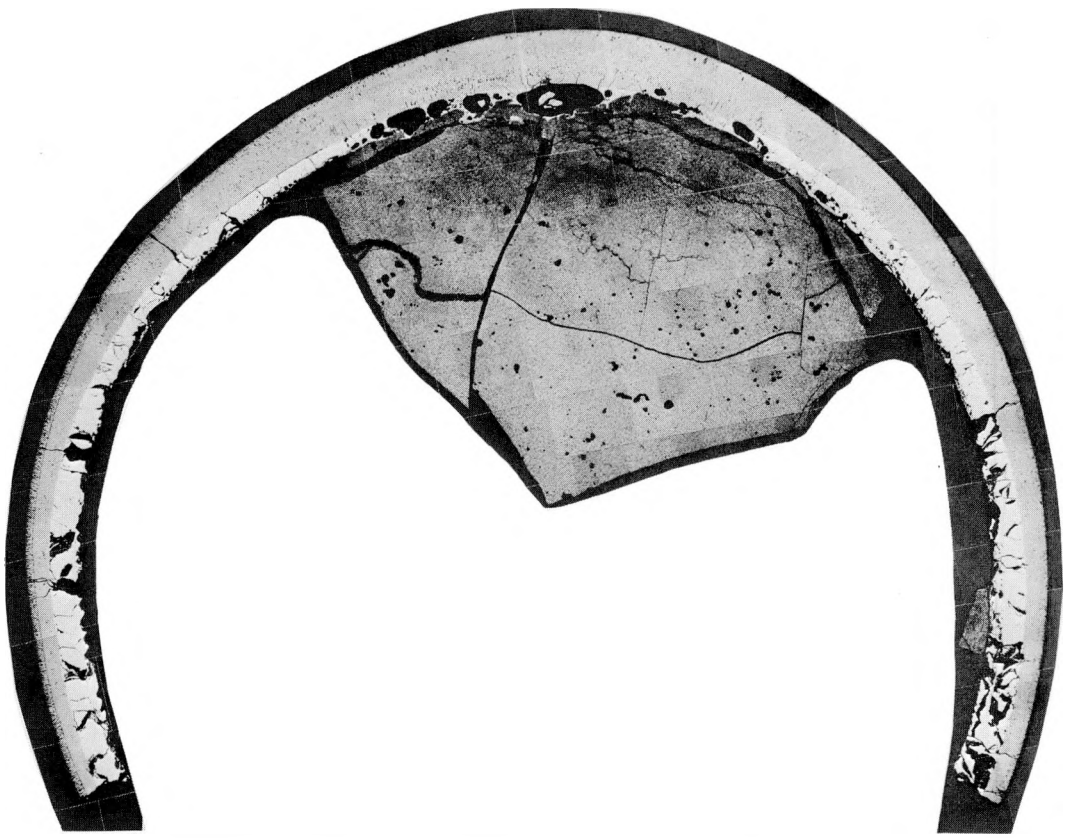

Fig. 14. Transverse Section through Fuel-containing Region of Cladding Segment Shown in Fig. 13. Neg. No. MSD-222389.

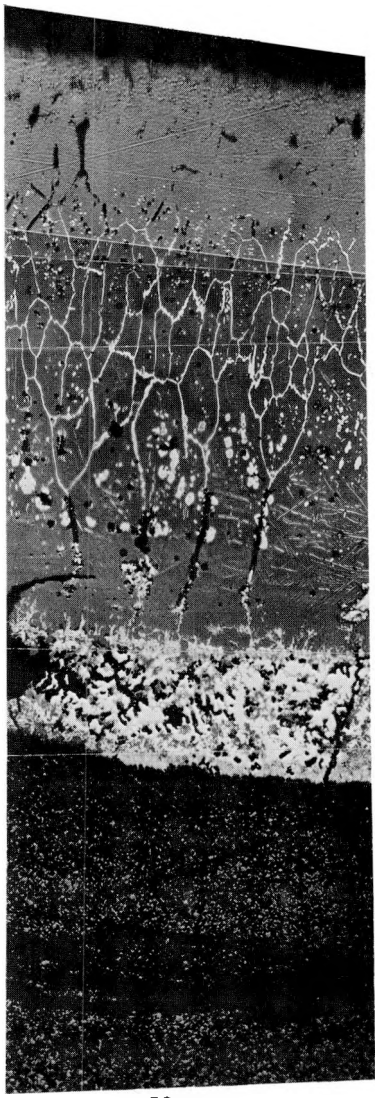

Fig. 15. Structure of Once-liquid Layer between Fuel and Oxidized Cladding. Test HT-2. Neg. No. 222573.

Adjacent to the oxide layer is a layer of large-grained metal, tentatively identified as oxygen-stabilized α Zircaloy. The combined thickness of the oxide and metal layers is ~64 mm, as compared with the original cladding thickness of 0.617 mm.

Microcracking in the fuel is most dense near the pellet periphery. Progressively fewer microcracks are observed as the center of the pellet is approached.

Between the fuel and cladding, a liquid or partially liquid layer formed. After solidifying, this layer apparently bonded the fuel chunks to the cladding. Several large gas bubbles, which were trapped within the liquid, are visible in Fig. 14. The once-liquid layer consists of at least two phases, one oxide and one metallic. The chemical compositions of the phases has not yet been determined. The multiple-phase structure of the once-liquid material is shown at higher magnification in Fig. 15. This morphology is considerably different from the once-liquid structures produced by annealing diffusion couples of UO_2 and Zircaloy at elevated temperatures.[10]

The further examination of the ORNL test specimens will be based on the preliminary results presented above. Particular attention will be focused in two areas: (1) fractographic examination of fuel using the scanning-electron microscope to determine whether bubble interlinkage processes played a role in fission-product release, and (2) electron microprobe examination to determine the composition of the phases in the once-liquid zone, diffusional interpenetration of uranium, oxygen, and zirconium, and the radial profile of cesium in selected fuel specimens.

References

1. J. Rest, *GRASS-SST: A Comprehensive, Mechanistic Model for the Prediction of Fission-gas Behavior in UO_2-base Fuels during Steady-state and Transient Conditions*, NUREG/CR-0202, ANL-78-53 (June 1978).

2. *Statistical Analysis System*, SAS Institute Inc., version SAS79.

3. R. A. Lorenz et al., *Fission Product Release from Highly Irradiated LWR Fuel*, NUREG/CR-0722, ORNL/NUREG/TM-287/R2 (Feb 1980).

4. A. P. Malinauskas, *Quarterly Progress Report on Fission Product Behavior in LWRs for the Period October-December 1978*, NUREG/CR-0682, ORNL/NUREG/TM-308 (Apr 1979).

5. A. P. Malinauskas, *Quarterly Progress Report on Fission Product Behavior in LWRs for the Period January-March 1979*, NUREG/CR-0917, ORNL/NUREG/TM-332 (Aug 1979).

6. S. M. Gehl, M. G. Seitz, and J. Rest, *Fission-gas Release from Irradiated PWR Fuel during Simulated PCM-type Accidents: Progress Report*, NUREG/CR-0088, ANL-77-80 (May 1978).

7. S. M. Gehl, *Comparison of Fission-gas Release and Mechanical Behavior during Transient Nuclear and Electrical Heating of Light-water-reactor Fuels*, NUREG/CR-1001, ANL-78-60 (June 1979).

8. M. O. Tucker, *Relative Growth Rates of Fission-gas Bubbles on Grain Faces*, J. Nucl. Mater. *78*, 17-23 (1978).

9. R. A. Lorenz, Oak Ridge National Laboratory, personal communication.

10. P. Hofmann and C. Politis, *The Kinetics of the Uranium Dioxide-Zircaloy Reactions at High Temperatures*, J. Nucl. Mater. *87*, 375-397 (1979).

Distribution for NUREG/CR-1801 (ANL-80-107)

Internal:

R. P. Anderson
R. Avery
E. S. Beckjord
M. Blander
Y. S. Cha
H. M. Chung
L. W. Deitrich
C. E. Dickerman
B. R. T. Frost
S. M. Gehl
E. E. Gruber
M. Ishii
W. D. Jackson
T. F. Kassner
A. B. Krisciunas
J. C. Leung
Y. Y. Liu
P. A. Lottes
W. E. Massey
L. McUmber
L. A. Neimark
R. G. Palm
D. R. Pepalis
R. B. Poeppel
J. Rest (30)
D. Stahl
E. M. Stefanski
R. P. Stein
C. E. Till
W. Wang
R. W. Weeks
J. B. Wozniak
F. L. Yaggee
ANL Contract File
ANL Libraries (2)
TIS Files (6)

External:

NRC, for distribution per R3 (400)
DOE-TIC(2)
Manager, Chicago Operations and Regional Office, DOE
Chief, Office of Patent Counsel, DOE-CORO
President, Argonne Universities Association
Materials Science Division Review Committee:
E. A. Aitken, General Electric Co., Sunnyvale
G. S. Ansell, Rensselaer Polytechnic Inst.
A. Arrott, Simon Fraser U.
R. W. Balluffi, Massachusetts Inst. Technology
S. L. Cooper, U. Wisconsin
C. Laird, U. Pennsylvania
M. E. Shank, Pratt & Whitney, East Hartford, Conn.
C. T. Tomizuka, U. Arizona
A. R. C. Westwood, Martin Marietta Labs.
R. B. Adamson, General Electric Co., Vallecitos Nuclear Center, P. O. Box 460, Pleasanton, Calif. 94566
J. Boulton, Whiteshell Nuclear Research Establishment, AECL, Pinawa, Manitoba, ROE 1LO, Canada
D. L. Burman, Westinghouse PWR Systems Div., P. O. Box 355, Pittsburgh, Pa. 15230
R. H. Chapman, Oak Ridge National Lab., P. O. Box X, Oak Ridge, Tenn. 37830
M. Charyulu, EG&G Idaho, Inc., P. O. Box 1625, Idaho Falls, Idaho 83401
F. D. Coffman, Div. of Operating Reactors, U. S. Nuclear Regulatory Commission, Washington
S. Dagbjartson, EG&G/INEL, 1520 Sawtelle Dr., Idaho Falls, Idaho 83401
J. Dearien, EG&G/INEL, 1520 Sawtelle Dr., Idaho Falls, Idaho 83401
D. Hagrman, EG&G/INEL, 1520 Sawtelle Dr., Idaho Falls, Idaho 83401
R. R. Hobbins, EG&G/INEL, 1520 Sawtelle Dr., Idaho Falls, Idaho 83401
D. O. Hobson, Oak Ridge National Lab., P. O. Box X, Oak Ridge, Tenn. 37830
W. V. Johnston, U. S. Nuclear Regulatory Commission, Washington
K. R. Jordan, Nuclear Fuel Div., Monroeville Nuclear Center, Westinghouse Electric Corp., Monroeville, Pa. 15146
P. MacDonald, EG&G/INEL, 1520 Sawtelle Dr., Idaho Falls, Idaho 83401
S. McDonald, Westinghouse Electric Corp. R&D Center, Beulah Rd., Pittsburgh, Pa. 15235
K. R. Merckx, Exxon Nuclear, Inc., 2955 George Washington Way, Richland, Wash. 99352

R. Mulgreen, Office of Nuclear Regulatory Research, U. S. Nuclear Regulatory Commission, Washington (3)
D. R. O'Boyle, Commonwealth Edison Co., P. O. Box 767, Chicago, Ill. 60690
H. Ocken, Electric Power Research Inst., P. O. Box 10412, Palo Alto, Calif. 94304
R. N. Oehlberg, Electric Power Research Inst., P. O. Box 10412, Palo Alto, Calif. 94304
T. P. Papazoglou, Lynchburg Research Center, Babcock & Wilcox Co., P. O. Box 1260, Lynchburg, Va. 24505
M. Picklesimer, U. S. Nuclear Regulatory Commission, Washington
D. Powers, Div. of Systems Safety, U. S. Nuclear Regulatory Commission, Washington
W. J. Quapp, EG&G/INEL, 1520 Sawtelle Dr., Idaho Falls, Idaho 83401
C. Ronchi, Euratom - T.V., Postfach 2266, 75 Karlsruhe, West Germany
P. Smerd, Combustion Engineering, Inc., P. O. Box 500, Windsor, Conn. 06095
V. W. Storhok, Battelle Columbus Labs., 505 King Ave., Columbus, O. 43201
R. A. Watson, Carolina Power and Light Co., P. O. Box 1551, Raleigh, N. C. 27602